Photoacoustic Imaging in Evaluating Early Intestinal Ischemia and Reperfusion Injury with Rat Models

Rui Wang
Yunnan Cancer Hospital
Teng Pan
University of Electronic Science and Technology
Lin Huang
University of Electronic of Science and Technology
Chengde Liao
Yunnan Cancer Hospital
Qinqing Li
Yunnan Cancer Hospital
Huabei Jiang
University of South Florida
Jun Yang (imdyang@qq.com)
Yunnan Cancer Hospital

Research article

Keywords: Photoacoustic imaging, Acute mesenteric ischemia, Intestinal tissue viability, Ischemia reperfusion

Posted Date: November 5th, 2020

DOI: https://doi.org/10.21203/rs.3.rs-94473/v1

Abstract

Purpose: It is still a challenge to distinguish whether the damaged intestine is viable or not in the treatment of acute mesenteric ischemia. In this study, photoacoustic imaging (PAI) was used to observe the activity of intestinal tissue after ischemia and reperfusion injury in rats.

Methods: With the approval of animal ethics committee our university, in vivo study was carried out. Forty male SD rats were randomly divided into four groups: sham operated (SO) group, 1 h ischemia group, 2 h ischemia group and ischemia-reperfusion (I/R) group. In the ischemia group, superior mesenteric artery (SMA) was isolated and clamped for 1 h (n = 10) and 2 h (n = 10), respectively. In I/R group, after ischemia for 1 hour, the clamp was removed and reperfused for 1 hour (n = 10). The same time interval of SMA was taken as SO group (n = 10). Immediately after the establishment of the animal model, PAI examination was performed. After PAI examination, the small intestine was collected for histopathology.

Results: The PAI derived parameters of 2 h ischemia group were significantly different from those of SO group and I/R group ($P < 0.05$). The levels of Hb, HbR, map760 and map 840 were increased in different degrees in ischemia group, especially in 2 h ischemia group (compared with SO group, $P < 0.01$). With the prolongation of ischemia time, the injury was aggravated. In immunohistochemistry, compared with SO group, BAX increased significantly in 2 h ischemia group ($P < 0.01$). Similarly, Caspase-3 was significantly higher than the baseline level ($P < 0.05$). The level of HIF-1a increased in 2 h ischemia group and I/R group ($P < 0.05$). TUNEL staining showed that the number of apoptotic positive nuclei in 2 h ischemia group was significantly higher than that in SO group ($P < 0.05$). HE staining showed that ischemia for 2 hours was the most serious, with obvious mucosal damage, extensive epithelial injury and bleeding.

Conclusions: PAI can be used as an effective tool to detect acute intestinal ischemia injury and quantitatively evaluate tissue viability.

Introduction

Intestinal ischemia and reperfusion (I/R) injury affects multiple groups of patients with different ages and complications, and has a high rate of morbidity and mortality[1]. This phenomenon occurs in many diseases, such as arterial embolism, strangulated hernia, colon cancer, volvulus, toxemia, mesenteric dysfunction and hypovolemic shock, which may lead to intestinal ischemia and reperfusion[2]. After ischemia injury, intestinal mucosa is characterized by excessive cell death and loss of barrier function[3]. Patients may rapidly decompensate, and then progress to sepsis and multiple system organ failure[4].

It is important to identify and locate damaged tissues before seriously intestinal injury occurs, as it allows surgeons to respond immediately[5]. At present, the assessment of tissue viability depends on the surgeon's expertise, but in practice, surgeons can only rely on the pulse and color of the intestine to estimate tissue perfusion and oxygen saturation[6]. In particular, the ischemic area should be accurately judged during operation to avoid over resection of ischemic small intestine. Although conventional

computed tomography (CT) and magnetic resonance imaging (MRI) can diagnose most intestinal diseases, they could not evaluate the hemodynamics and microcirculation blood flow of the lesions, which affect the accurate clinical stage, treatment and evaluation of curative effect. Therefore, for intestinal diseases, especially intestinal ischemia, it is necessary not only to make morphological diagnosis by CT and MRI, but also to further evaluate the abnormality of intestinal blood flow[7, 8]. Several other commonly used detection techniques, such as sidestream dark field imaging[9], spectrophotometry and laser Doppler blood flow measurement, have been used to study intestinal microcirculation[10]. However, these techniques are either not sensitive enough or not clinically available to detect rapid changes in intestinal permeability in vivo.

Since there is no effective method to achieve the reliability and repeatability of the results expected, we proposed to apply photoacoustic imaging (PAI) to this problem. PAI is a hybrid imaging method that combines optical contrast and ultrasonic resolution[11, 12]. It combines high-resolution volume imaging of tissue depths from a few millimeters to centimeters with the ability to analyze drugs with molecular specificity, vascular system and physiological parameters[13]. PAI is particularly suitable for vascular imaging because of the high concentration of hemoglobin in the blood, which can achieve strong absorption, so it has a high contrast with surrounding tissues[14, 15]. These unique functions provide a theoretical basis for gastrointestinal PAI. To evaluate the changes of gastrointestinal anatomy and function, it is important to detect accurately by multi wavelength method[16]. At present, the application of PAI technology to evaluate intestinal ischemia and reperfusion injury has not been fully studied.

In this paper, we hypothesized that PAI could be used to evaluate intestinal ischemia and reperfusion injury. Therefore, the purpose of this study is to explore the characteristics of photoacoustic signal changes in rat model of acute mesenteric ischemia and reperfusion injury by PAI, and to make histopathological analysis.

Materials And Methods

Animals

All animal protocols used in this study were approved and monitored by the Animal Ethics Committee of Kunming Medical University. Adult male Sprague Dawley (SD) rats weighing 180 ~ 200 g were selected in the experiment. The animals were fed in a temperature-controlled room (20 ± 2 °C) for 12 hours in a light and dark circulation. Before PAI, the animals were fasted for 12 hours but drank freely.

Experimental Protocols

40 SD rats were randomly divided into sham-operation group (SO), 1 h ischemia group, 2 h ischemia group and ischemia-reperfusion group (IR). Before the experiment, rats fasted overnight and drank freely. The experimental process was carried out under aseptic condition. Anesthesia was performed by intraperitoneal injection of 10% chloral hydrate (1.2 g/kg), followed by a midline laparotomy in order to

obtain abdominal exposure. After identifying the small intestine and cecum, the superior mesenteric artery (SMA) was carefully exposed. The root of SMA was separated and occluded with noninvasive microvascular forceps. The gauze pad is placed on the intestinal tract and is often wetted with warm saline water. After 1 h of ischemia, the clamp was removed and reperfused for 1 h to establish the ischemia-reperfusion model of SMA (n = 10). In the ischemia group, SMA was separated and clamped for 1 h (n = 10) and 2 h (n = 10), and no longer perfused. SO group (n = 10) was used as control group, SMA was separated but not clamped after operation, and compared with corresponding IR group. Before PAI examination, laid intestines on the surface of the imaging cavity, and smoothed the intestines with a cotton swab. Poured the stirred ultrasound agent into the cavity and smoothed the surface of the couplants with a cotton swab until it was flush with the probe surface. The three intestinal parts of each rat were imaged at 780 nm and 840 nm respectively, and the signal of each image was averaged 10 times to reduce noise.

PAI System

Experimental system for dynamic monitoring of intestinal ischemia and reperfusion injury was shown in Fig. 1. A Q-switched Nd:YAG laser (Surelite, Continuum, California) emits light with a wavelength of 532 nm, which is transformed into 700–960 nm after passing through an optical parametric oscillator (OPO). After the output laser passes through the two mirrors, the horizontal light path relative to the ground is adjusted to be vertically downward. Before irradiating the biological tissue, the light passes through a ground glass to increase the imaging area; in the process of collecting the signal, the ground glass is removed, and the light directly illuminates on the tissue. The incident fluence at 760 nm was estimated to be 5 mJ/cm2, which is below the ANSI safety. A 128-element concave ultrasound transducer array (Japan Probe Co., Ltd., Japan) was used to receive photoacoustic signals. A custom-built 128-channel preamplifier (60 dB) was connected to the probe, and the amplified PA signals were transferred to a 64-channel analog-to-digital system (PXIe5105; NI. Inc).

Image Reconstruction and Data Processing

The images were reconstructed by the delay-and-sum algorithm. The intensity of the photoacoustic signal is directly related to the absorption of NIR light by tissues, among which hemoglobin and melaninare the main absorption substances. In order to define the region of interest (ROI), PAI signal pixel values greater than 0.6 times the maximum signal were selected. As shown in Fig. 5, the ROI was exactly the part of the mesenteric blood vessels, where the blood perfusion change was obvious during ligation and reperfusion. After ROI is determined, dual wavelength image signals are used to calculate total hemoglobin and deoxidized and oxyhemoglobin content.

Histopathology

Hematoxylin-Eosin (HE)

After PAI, the animals were killed at different time points after operation, 100 ml normal saline containing heparin was perfused through the heart, and then 100 ml 4% paraformaldehyde was injected. The tissue

samples were fixed in 10% formalin solution and then dehydrated overnight in 30% sucrose. Embedded in paraffin, 5 μ m slices were cut by slicing machine. It is then dried overnight in an incubator at 45 ° C. The sections were further stained with hematoxylin-eosin (HE) and observed under light microscope.

Western blot

As mentioned previously, the small intestinal tissue was scraped and homogenized in a 10 fold volume of cold RIPA buffer. After incubation on ice for 30 minutes, the cell lysate was centrifuged at 14000 rpm for 15 minutes, and the protein concentration in the supernatant was determined. The supernatant was dissolved in 2 × electrophoresis sample buffer at a ratio of 1:1, subjected to high temperature heat sealing, and stored at − 20 ℃ for use. The extracted proteins were separated by twelve alkyl sulphate polyacrylamide gel electrophoresis with different concentrations, and the separated proteins were electrotransferred to poly vinylidene fluoride two membrane. Sealed with 5% non-fat milk, incubated overnight with primary antibody at 4 °C, and then incubated with horseradish peroxidase labeled secondary antibody at room temperature for 1 h. Specific proteins including cleaved Caspase-3, Bcl-2, Bax and HIF-1α were observed with enhanced chemiluminescence enhancement kits. The following antibodies were used: rabbit anti-Cleaved Caspase-3 (#9664, Cell Signaling Technology,), anti-bcl-2 antibody (ab59348, Abcam), Bax Antibody (#2772, Cell Signaling Technology), rabbit anti-HIF-1α (#14179, Cell Signaling Technology). The band density was observed by gel electrophoresis imaging system and quantified by ImageJ software (https://imagej.nih.gov/).

TUNEL Staining

TUNEL method was used to identify apoptotic cells in tissue sections of double stranded DNA fragments. DNA fragments were labeled by enzyme immobilized nucleotides. In order to detect apoptosis, we used the apoptosis detection kit (In situ cell death detection kit-POD, Roche). The sample was rehydrated in alcohol and then immersed in phosphate buffered saline (PBS) at room temperature for 5 minutes. The tissues were treated with proteinase K solution for 15–20 minutes and washed twice with PBS at 21–37 ° C. The TUNEL reaction mixture was prepared and the slide was immersed in 1 × TDT labeled buffer for 5 minutes. After stopping the labeling reaction, the samples were covered with diluted anti BrdU and cultured at 37 ° C for 1 hour. Cover with horseradish peroxidase solution for 10 minutes and immerse in diaminobenzidine solution for 5 minutes. Then, under the fluorescence microscope, the number of positive cells in each slide was counted and the average fluorescence intensity was calculated.

Statistical Analysis

All biochemical indexes were expressed as mean ± standard deviation, and were compared by single factor and multi factor analysis of variance. Spearman correlation coefficient was used to analyze the correlation between perfusion parameters and biochemical indexes. SPSS 23.0 software (SPSS, Inc., Chicago, IL, USA) was used for statistical analysis. After statistics, *P* value less than 0.05 was considered to have statistically significant.

Results

The signal intensity of PAI in intestine injury

After the light passes through the ground glass, the irradiated area becomes larger, and most of the tissue of the intestine in the phantom cavity can be observed. Figure 2 showed one of the photoacoustic images of the intestines of a SD rat in the control group using PAI system. Figure 2a is the image of rat intestinal tissue, and 2b is the corresponding photoacoustic reconstruction image. The yellow circle in the lower right corner is the enlarged detail. As shown in the photoacoustic image, the border of the intestine was outlined, and several mesenteric blood vessels and even capillaries were clearly visible. The area in the middle of the image is significantly brighter than the tissue at the edges, due to uneven illumination.

When the ground glass is removed, the light is irradiated on the tissue with a more concentrated energy and a smaller spot, but at the cost of reducing the imaging area. The position of the light spot can be moved two-dimensionally by the adjusters on the mirror mount, so that the light can irradiate different intestinal areas of interest. Therefore, the intestinal tissue of a rat can be divided into 3–4 areas and imaged separately, thereby concentrating light energy and increasing the number of samples.

PAI parameters of each group were shown in Fig. 3. There was no significant change in PAI signal parameters of normal small intestine. But, PAI signal in experimental group was almost stronger than that in SO group. In general, the levels of Hb, HbR, MAP 760 and MAP 840 in the ischemia group increased with varying degrees, especially in the 2 h ischemia group ($P < 0.01$). With the prolongation of ischemia time, the injury was aggravated. The levels of Hb and MAP 840 at 1 h after ischemia were higher than those in SO group, but the difference was not statistically significant ($P > 0.05$). The level of MAP 760 in each experimental group was significantly higher than that in SO group ($P < 0.05$). There was no significant difference in HbO and oxygen saturation (sO2) between experimental and control groups. Compared with SO group, all PAI signal levels increased except HbO. Among them, it increased 1.01–1.50 times in 1 h ischemia group, 1.30-1.59-fold in 2 h ischemia group, and 1.01-1.38-fold in I/R group.

Hematoxylin eosin staining

Hematoxylin eosin staining of small intestine sections is shown in the Fig. 4. In the SO group, the villi of small intestine were arranged orderly, the cell size and extracellular space were consistent, and there was no obvious inflammatory cell infiltration. Swelling and congestion of intestinal villi and exfoliation of epithelial cells were found in 1 h and 2 h injury groups. In addition, obvious mucosal injury, extensive epithelial injury, lamina propria disintegration and hemorrhage were observed in 2 h ischemia group.

Ischemia induced Caspase-3, BAX, Bcl-2 and HIF-1α expression in intestines

Compared with SO group, the expression of Cleaved Caspase-3 in ischemia group and reperfusion group continued to increase. The level of Cleaved Caspase-3 in 2 h ischemia group and I/R group was significantly higher than the baseline value ($P < 0.05$). BAX showed increase in the experimental group, which only slightly increased in the 1-hour ischemia group (compared with the SO group, $P > 0.05$), but

significantly increased in the 2-hour ischemia group ($P < 0.01$). The expression levels of Bcl-2 in ischemia group and I/R group were lower than those in so group, but the difference was not statistically significant ($P > 0.05$). The expression of HIF-1a increased gradually in the experimental group. Compared with SO group, HIF-1a level was increased in 2 h ischemia group and I/R group. ($P < 0.05$) (Fig. 5)

TUNEL staining

TUNEL staining was used to identify apoptotic nuclei induced by ischemia and reperfusion. In the SO group, a small number of TUNEL positive nuclei were found in the intestine. The ischemia injury induced by SMA hemostatic clip increased the number of TUNEL positive nuclei. In addition, the number of TUNEL positive nuclei in 2 h ischemia group was significantly higher than that in SO control group ($P = 0.03$). (As shown in Fig. 6)

Discussion

Evaluation of intestinal tissue viability is key to the treatment of acute mesenteric ischemia. Surgeons are often faced with a very difficult choice, especially in surgery. Extensive intestinal resection may cause serious complications such as short bowel syndrome[17]. However, if the necrotic part of the intestinal resection is not sufficient, it may lead to severe systemic inflammatory response, and even induce multiple organ dysfunction[18]. Therefore, accurate judgment of the range of the involved bowel is very important for the success of the operation. At present, there is no certain standard for judging intestinal viability. In recent years, fluorescein, Doppler, electromyographyand, radionuclide have been used to determine intestinal vitality[19–21]. However, its wide application is limited by the complexity of operation methods, the use of special instruments and the high cost of inspection. CT and MRI are also used to predict or measure intestinal viability, and have certain diagnostic value for intestinal ischemia injury[22, 23]. However, these imaging techniques usually produce motion artifacts due to the patient's heartbeat and respiration[24]. Most importantly, these devices cannot be used during surgery. In the operation, the surgeon's experience can only be used to judge the severity of intestinal injury, so as to determine the scope of operation, which is a subjective judgment method. PAI is an objective evaluation method and can be used for quantitative analysis to reflect the changes of pathophysiology. Furthermore, this method can be used for real-time imaging during operation.

Compared with the conventionally used clinical evaluation methods of intestinal ischemia and reperfusion (such as CT or MRI), the method used in this paper was not affected by motion artifacts and tissue thickness was up to several millimeters. PAI is a non-destructive medical imaging method. It combines the high contrast characteristics of pure optical imaging and the high penetration depth characteristics of pure ultrasound imaging, which can provide high resolution and high contrast tissue imaging. In our experiment, the mesenteric artery we interested in was only a few millimeters below the surface of the irradiated tissue, and under proper illumination, the tissue depth could even be within cm (depending on the irradiated organ)[25]. In addition, when using a single acquisition mode, PAI can be considered instantaneous (usually completed in tens of milliseconds), which means no motion artifacts

are generated[26, 27]. More importantly, since the reconstruction is real-time, movement within the illumination area between the tissues does not affect the repeatability or accuracy of the method. With this method, we can directly measure the degree of ischemia of intestinal vessels and quantitative information of blood reperfusion, with a resolution of up to 5 μm.

In this study, we used histopathological results to verify whether PAI in intestinal tissue can assess tissue viability. As described in the results, PAI detected changes in intestinal tissue viability associated with intestinal ischemia time in a model of acute mesenteric ischemia injury. It is noteworthy that the signal intensity of small intestine in 2 h ischemia group was significantly increased, which was 1.30–1.59 times of that in control group. PAI indirectly explained that the blood circulation near the injured intestine was much higher than that in the normal intestine, as expected by acute inflammation. Villi edema, epithelial cells shedding, tissue edema, congestion and bleeding were observed in ischemia group, blood vessels and lymphatic vessels were obviously dilated, and glands were damaged. Moreover, with the prolongation of ischemia time, the degree of injury was obviously aggravated. The results showed that intestinal ischemia could significantly increase the apoptosis rate of intestinal mucosal cells. With the increase of intestinal ischemia time, apoptosis also increased, and it was the most serious in 2 h ischemia group. Bcl-2 is an important protein in the study of apoptosis[28]. We found that intestinal ischemia could significantly reduce the expression level of Bcl-2. With the prolongation of intestinal ischemia time, the levels of Bcl-2 decreased, and the lowest in I/R group. On the contrary, the expression of Bax increased in the experimental group, and the highest level was found in 2 h ischemia group. The level of Caspase-3 was significantly higher than that of control in 2 h ischemia group. TUNEL staining is a combination of molecular biology and morphology. In situ staining of single apoptotic nucleus or apoptotic body can accurately reflect the most typical biochemical and morphological characteristics of apoptosis. In the experimental group, we observed that TUNEL staining showed that apoptosis was the most serious in 2 h ischemia group. In addition to observing the indexes of apoptosis, we also observed the indexes related to hypoxia status. HIF-1α reflects the hypoxia state of tissues, and the expression level of HIF-1α in the experimental group showed an upward trend. HIF-1α is an important transcriptional regulator that mediates cell involvement in hypoxia response. The increased expression of HIF-1α indicates severe hypoxia and reflects tissue hypoxia[29]. We found that HIF-1α level was significantly increased in 2 h ischemia group, indicating that hypoxia was severe in this group. At the same time, the levels of Hb, HbR and MAP760 in this group were significantly higher than those in the control group. Photoacoustic parameters directly indicate the change of oxygen content in tissues[30]. Through the histopathological examination of tissue samples, the results of this study show that PAI technology can quickly and real-time assess the degree of intestinal ischemia injury in the experimental model.

In the process of ischemia and reperfusion, there is a dependence between reperfusion injury and ischemia time, and the ischemia process itself can cause injury, which is also the basis of reperfusion injury[31, 32]. The essence of reperfusion injury is to further aggravate or convert the injury in ischemic phase into irreversible injury after blood flow recovery[33]. So the first thing that affects reperfusion injury is ischemia time[34]. The ischemia time is short, and there is no obvious reperfusion injury after the blood

supply is restored, because all organs can tolerate a certain period of ischemia. If the ischemia time is long, the recovery of blood supply will easily lead to reperfusion injury. It has been reported that most of the ischemia and reperfusion time is 1 hour, which can make a more ideal intestinal I/R model[35]. In addition, in our experimental group, we found that there was no significant difference in PAI between the 1 h ischemia group and the SO group, suggesting that intestinal ischemia may be reversible at this time. The histopathological findings were similar, and there is no significant difference between the two groups, which may be due to the mild apoptosis and tissue ischemia. In this study, the application of PAI after intestinal ischemic injury in rats was evaluated in vivo and in real time. Small bowel imaging requires a visual field of about 3–4 cm in diameter and a resolution of up to 200 mm to accurately observe the vascular system. And we use the PAI system, which can provide the required resolution and field of view. The results show that PAI can reflect the pathophysiological changes of the intestine, such as apoptosis and hypoxia, to judge the intestinal vitality. It is helpful for surgeons to evaluate ischemic injury objectively during living body surgery.

In previous experimental I/R model, the observation of intestinal viability loss was usually limited to long-term ischemia (3 hours after injury)[36, 37]. After ischemic injury, the study of monitoring intestinal permeability in vitro showed that it took at least 60 minutes to detect the change of intestinal barrier function, which could not quickly judge the change of intestinal viability[3]. PAI breaks the limitation of the previous technology, and uses its real-time detection technology to detect intestinal injury quickly, which provides a means for early diagnosis and early targeted treatment of injury in the future. The strong light absorption of hemoglobin in tissues makes the blood vessels have a very high contrast in photoacoustic images, which is also the basis for PAI technology to detect hemoglobin content[38]. The light absorption detected by PAI is the result of complex interaction between blood volume and oxygen consumption. Ischemia usually reduces part of the intestinal blood volume and oxygenation, which directly leads to a decrease in tissue absorption characteristics[39]. Spectral analysis of PAI images showed that there were significant differences in PAI images between the experimental models with different ischemic time, and the degree of ischemic injury could be judged by PAI. In our experiment, PAI parameters at different wavelengths can reflect the corresponding morphological and histological changes of intestinal tract.

Our research has some limitations. Firstly, the intestinal I/R model with mesenteric artery ligation can not fully simulate clinical intestinal ischemia. Although complete intestinal ischemia may be secondary to mesenteric artery thrombosis or embolus, most of the ischemic attacks are caused by segmental ischemia, such as intestinal adhesion obstruction or incarcerated hernia[40]. Nevertheless, the mesenteric artery ligation model simulates the most severe intestinal ischemia and may be the best animal model to test the effectiveness of the new therapy. Secondly, although our results are expected to be used for intraoperative or laparoscopic detection, it needs to rely on the penetration of light at a deeper depth if it is to be used for in vitro examination, because molecules such as water and protein in skin and muscle will greatly reduce the light energy of deep tissue[41]. In the future, we will continue to study these issues.

Conclusions

In this study, PAI was used to study the extent of intestinal ischemia injury in rat models. Our findings indicate that PAI can determine the severity of ischemic injury and reflect the changes of histopathology. Therefore, PAI may provide surgeons with a more reliable and accurate method to evaluate intestinal tissue viability in ischemic injury.

Abbreviations

PAI: Photoacoustic imaging; SMA: Superior mesenteric artery; I/R: Ischemia and reperfusion; CT: Computed tomography; MRI: Magnetic resonance imaging; SD: Sprague Dawley; SO: Sham-operation; OPO: Optical parametric oscillator; ROI: Region of interest; HE: Hematoxylin-Eosin; PBS: Phosphate buffered saline

Declarations

Acknowledgements

Not applicable.

Authors' contributions

JY and HBJ designed this study. RW, TP, and LH performed the experiments. QQL collected and analyzed the data. RW and TP wrote the manuscript, which was critically reviewed and revised by CDL. All of the authors read and approved the final manuscript.

Funding

This study was supported by the National Natural Science Foundation of China (NSFC Grants 82060313 to J.Y.).

Availability of data and materials

The datasets used or analyzed during the current study are available from the corresponding author on reasonable request.

Ethics approval and consent to participate

The study protocol was approved by the Animal Ethics Committee of Kunming Medical University.

Consent for publication

Not applicable.

Competing interests

The authors declare that they have no competing interests.

References

1. Nadatani Y, Watanabe T, Shimada S, et al. Microbiome and intestinal ischemia/reperfusion injury. *J Clin Biochem Nutr.* 2018;63:26-32.
2. Eryilmaz S, Turkyilmaz Z, Karabulut R, et al. The effects of hydrogen-rich saline solution on intestinal anastomosis performed after intestinal ischemia reperfusion injury. *J Pediatr Surg.* 2019.
3. Hsiao JK, Huang CY, Lu YZ, et al. Magnetic resonance imaging detects intestinal barrier dysfunction in a rat model of acute mesenteric ischemia/reperfusion injury. *Invest Radiol.* 2009;44:329-335.
4. Jensen AR, Doster DL, Hunsberger EB, et al. Human Adipose Stromal Cells Increase Survival and Mesenteric Perfusion Following Intestinal Ischemia and Reperfusion Injury. *Shock.* 2016;46:75-82.
5. Struck R, Wittmann M, Muller S, et al. Effect of Remote Ischemic Preconditioning on Intestinal Ischemia-Reperfusion Injury in Adults Undergoing On-Pump CABG Surgery: A Randomized Controlled Pilot Trial. *J Cardiothorac Vasc Anesth.* 2018;32:1243-1247.
6. Mariani P, Slim K. Enhanced recovery after gastro-intestinal surgery: The scientific background. *J Visc Surg.* 2016;153:S19-S25.
7. Shi H, Li R, Qiang J, et al. Computed Tomography Perfusion Imaging Detection of Microcirculatory Dysfunction in Small Intestinal Ischemia-Reperfusion Injury in a Porcine Model. *PLoS One.* 2016;11:e0160102.
8. Zhao DW, Zhang LT, Cheng HY, et al. Monitoring dynamic alterations in calcium homeostasis by T1-mapping manganese-enhanced MRI (MEMRI) in the early stage of small intestinal ischemia-reperfusion injury. *NMR Biomed.* 2015;28:958-966.
9. Lehmann C, Abdo I, Kern H, et al. Clinical evaluation of the intestinal microcirculation using sidestream dark field imaging--recommendations of a round table meeting. *Clin Hemorheol Microcirc.* 2014;57:137-146.
10. Dima A, Gateau J, Claussen J, et al. Optoacoustic imaging of blood perfusion: techniques for intraoperative tissue viability assessment. *J Biophotonics.* 2013;6:485-492.
11. Zhang S, Qi L, Li X, et al. Photoacoustic imaging of living mice enhanced with a low-cost contrast agent. *Biomed Opt Express.* 2019;10:5744-5754.
12. Knieling F, Gonzales Menezes J, Claussen J, et al. Raster-Scanning Optoacoustic Mesoscopy for Gastrointestinal Imaging at High Resolution. *Gastroenterology.* 2018;154:807-809 e803.
13. Qin W, Qi W, Xi L. Quantitative investigation of vascular response to mesenteric venous thrombosis using large-field-of-view photoacoustic microscopy. *J Biophotonics.* 2019;12:e201900198.
14. Karlas A, Kallmayer M, Fasoula NA, et al. Multispectral optoacoustic tomography of muscle perfusion and oxygenation under arterial and venous occlusion: A human pilot study. *J Biophotonics.* 2020;13:e201960169.
15. Bayer CL, Wlodarczyk BJ, Finnell RH, et al. Ultrasound-guided spectral photoacoustic imaging of hemoglobin oxygenation during development. *Biomed Opt Express.* 2017;8:757-763.

16. Petrov YY, Petrova IY, Patrikeev IA, et al. Multiwavelength optoacoustic system for noninvasive monitoring of cerebral venous oxygenation: a pilot clinical test in the internal jugular vein. *Opt Lett.* 2006;31:1827-1829.
17. Turato WM, Sales-Campos H, Braga CB, et al. The impact of intestinal resection on the immune function of short bowel syndrome patients. *Hum Immunol.* 2016;77:1202-1208.
18. Osuka A, Kusuki H, Matsuura H, et al. Acute intestinal damage following severe burn correlates with the development of multiple organ dysfunction syndrome: A prospective cohort study. *Burns.* 2017;43:824-829.
19. Li T, Tomimatsu T, Ito K, et al. Fluorescein-methotrexate transport in brush border membrane vesicles from rat small intestine. *Life Sci.* 2003;73:2631-2639.
20. Sugito K, Kusafuka T, Hoshino M, et al. Usefulness of color doppler sonography and 99m Tc-RBC scintigraphy for preoperative diagnosis of a venous malformation of the small intestine in a 2-year-old child. *J Clin Ultrasound.* 2008;36:56-58.
21. Schiemer JF, Heimann A, Somerlik-Fuchs KH, et al. Five-fold Gastrointestinal Electrical Stimulation With Electromyography-based Activity Analysis: Towards Multilocular Theranostic Intestinal Implants. *J Neurogastroenterol Motil.* 2019;25:461-470.
22. Minhas AS, Sharkey J, Randtke EA, et al. Measuring Kidney Perfusion, pH, and Renal Clearance Consecutively Using MRI and Multispectral Optoacoustic Tomography. *Mol Imaging Biol.* 2020;22:494-503.
23. Tseng CY, Chang CM, Yang SC, et al. Spontaneous Intramural Intestinal Hemorrhage versus Acute Mesenteric Ischemia by CT Evaluation. *Intern Med.* 2016;55:2337-2341.
24. Copin P, Zins M, Nuzzo A, et al. Acute mesenteric ischemia: A critical role for the radiologist. *Diagn Interv Imaging.* 2018;99:123-134.
25. Ivankovic I, Dean-Ben XL, Lin HA, et al. Volumetric optoacoustic tomography enables non-invasive in vivo characterization of impaired heart function in hypoxic conditions. *Sci Rep.* 2019;9:8369.
26. Lediju Bell MA. Photoacoustic imaging for surgical guidance: Principles, applications, and outlook. *J Appl Phys.* 2020;128:060904.
27. Zhong Y, Zou Y, Liu L, et al. pH-responsive Ag2S nanodots loaded with heat shock protein 70 inhibitor for photoacoustic imaging-guided photothermal cancer therapy. *Acta Biomater.* 2020.
28. Anantram A, Degani M. Targeting cancer's Achilles' heel: role of BCL-2 inhibitors in cellular senescence and apoptosis. *Future Med Chem.* 2019;11:2287-2312.
29. Semenza GL. Targeting hypoxia-inducible factor 1 to stimulate tissue vascularization. *J Investig Med.* 2016;64:361-363.
30. Karmacharya MB, Sultan LR, Kirkham BM, et al. Photoacoustic Imaging for Assessing Tissue Oxygenation Changes in Rat Hepatic Fibrosis. *Diagnostics (Basel).* 2020;10.
31. Shiva N, Sharma N, Kulkarni YA, et al. Renal ischemia/reperfusion injury: An insight on in vitro and in vivo models. *Life Sci.* 2020;256:117860.

32. Sanchez-Hernandez CD, Torres-Alarcon LA, Gonzalez-Cortes A, et al. Ischemia/Reperfusion Injury: Pathophysiology, Current Clinical Management, and Potential Preventive Approaches. *Mediators Inflamm.* 2020;2020:8405370.
33. Soares ROS, Losada DM, Jordani MC, et al. Ischemia/Reperfusion Injury Revisited: An Overview of the Latest Pharmacological Strategies. *Int J Mol Sci.* 2019;20.
34. Schmucker RW, Mendenhall SD, Reichensperger JD, et al. Defining the Salvage Time Window for the Use of Ischemic Postconditioning in Skeletal Muscle Ischemia Reperfusion Injury. *J Reconstr Microsurg.* 2015;31:597-606.
35. Gubernatorova EO, Perez-Chanona E, Koroleva EP, et al. Murine Model of Intestinal Ischemia-reperfusion Injury. *J Vis Exp.* 2016.
36. Zhao L, Luo L, Chen J, et al. Utilization of extracorporeal membrane oxygenation alleviates intestinal ischemia-reperfusion injury in prolonged hemorrhagic shock animal model. *Cell Biochem Biophys.* 2014;70:1733-1740.
37. Boettcher M, Eschenburg G, Mietzsch S, et al. Therapeutic targeting of extracellular DNA improves the outcome of intestinal ischemic reperfusion injury in neonatal rats. *Sci Rep.* 2017;7:15377.
38. Tzoumas S, Nunes A, Olefir I, et al. Eigenspectra optoacoustic tomography achieves quantitative blood oxygenation imaging deep in tissues. *Nat Commun.* 2016;7:12121.
39. Li Z, Li H, Chen H, et al. In vivo determination of acute myocardial ischemia based on photoacoustic imaging with a focused transducer. *J Biomed Opt.* 2011;16:076011.
40. Cox VL, Tahvildari AM, Johnson B, et al. Bowel obstruction complicated by ischemia: analysis of CT findings. *Abdom Radiol (NY).* 2018;43:3227-3232.
41. Vogt WC, Jia C, Wear KA, et al. Biologically relevant photoacoustic imaging phantoms with tunable optical and acoustic properties. *J Biomed Opt.* 2016;21:101405.

Figures

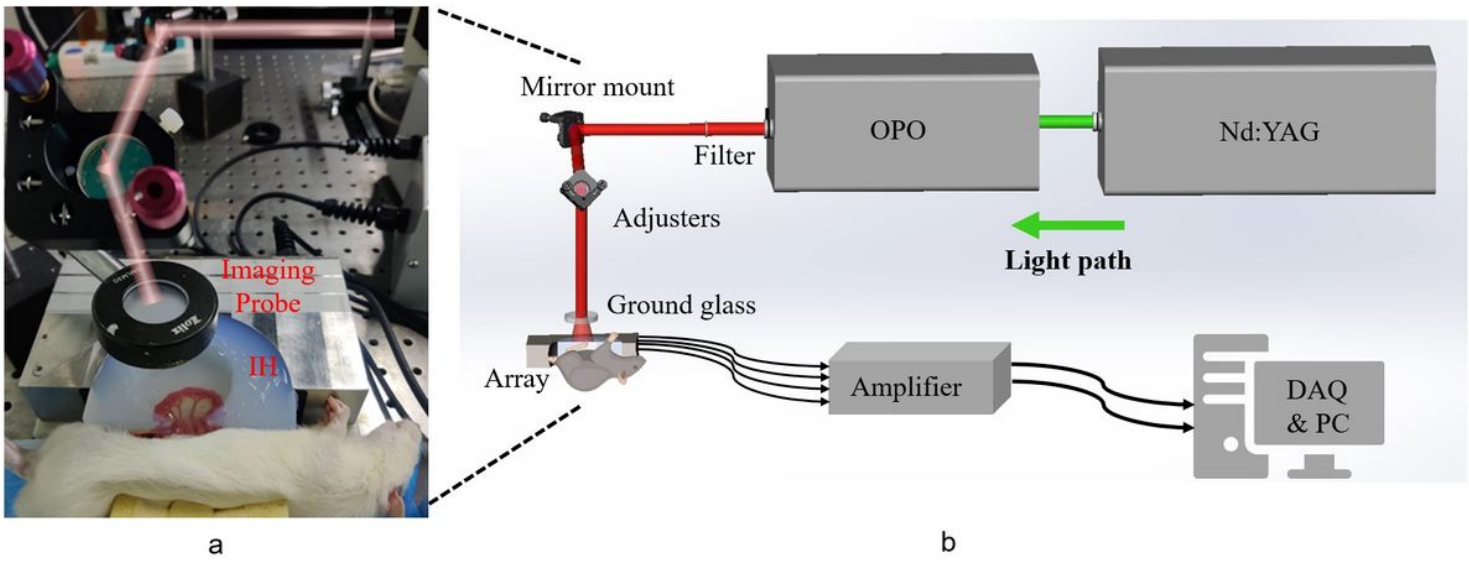

Figure 1

Schematic of the photoacoustic tomography system. (a) Detail of the imaging probe. (b) Schematic of the experimental setup. (DAQ, data acquisition; OPO, optical parametric oscillator; IH, Intestinal holder)

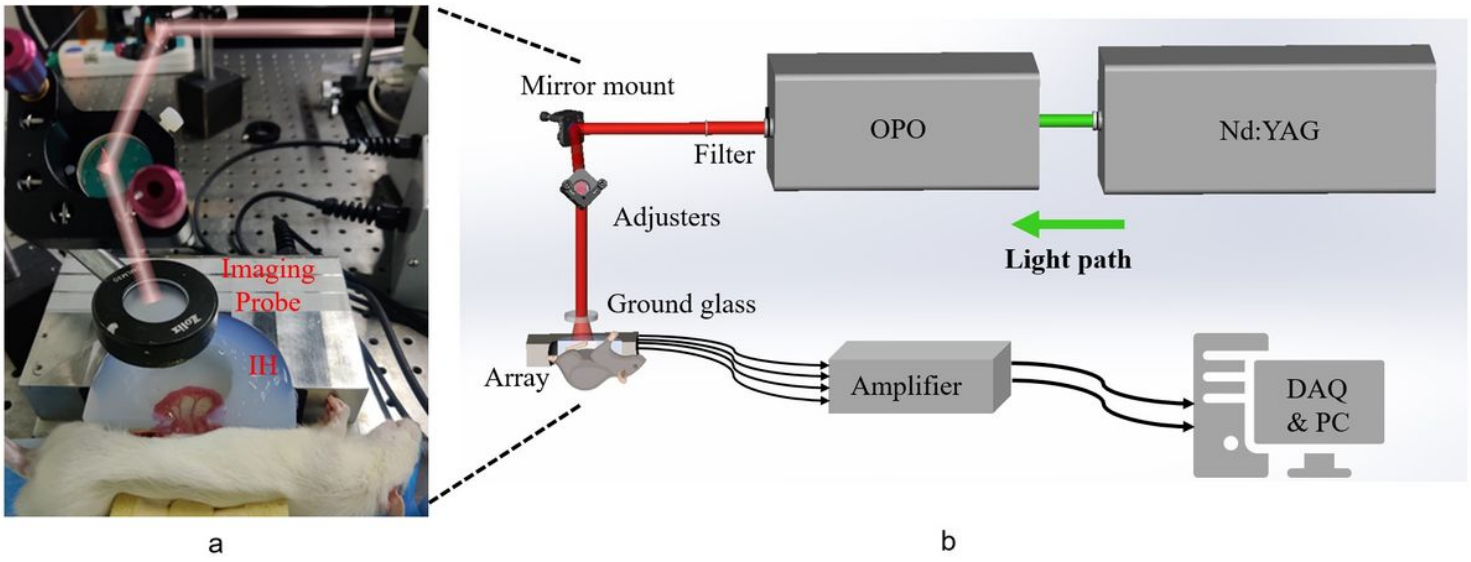

Figure 1

Schematic of the photoacoustic tomography system. (a) Detail of the imaging probe. (b) Schematic of the experimental setup. (DAQ, data acquisition; OPO, optical parametric oscillator; IH, Intestinal holder)

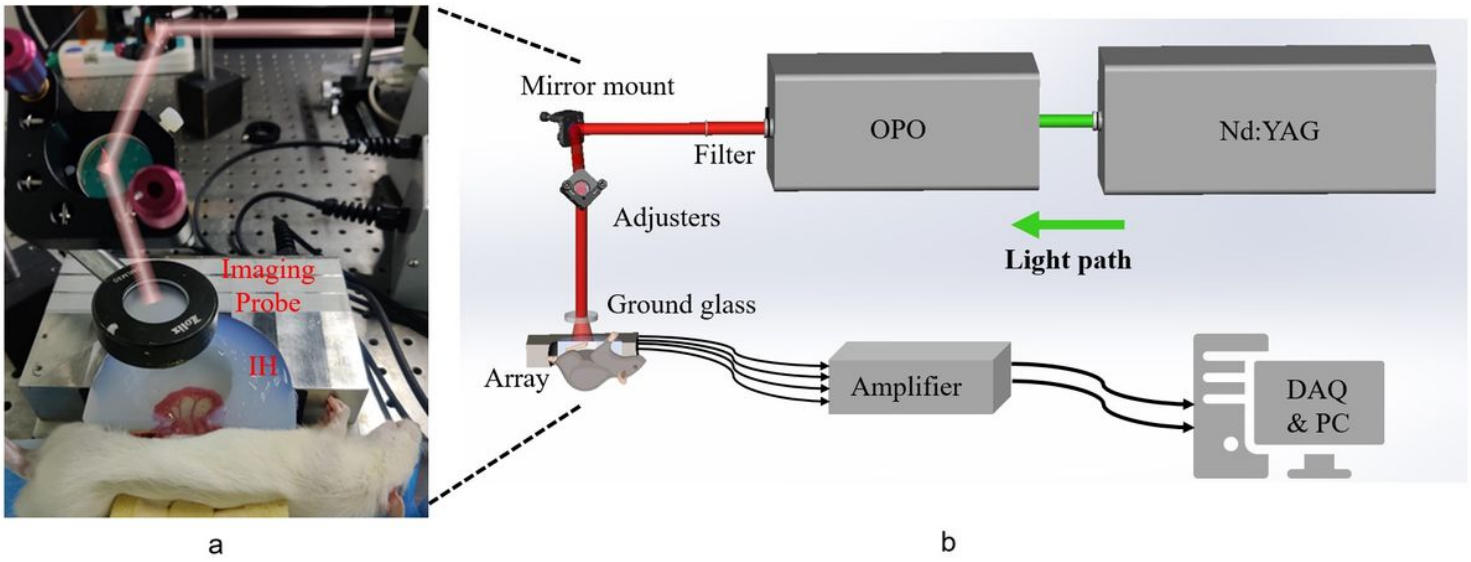

Figure 1

Schematic of the photoacoustic tomography system. (a) Detail of the imaging probe. (b) Schematic of the experimental setup. (DAQ, data acquisition; OPO, optical parametric oscillator; IH, Intestinal holder)

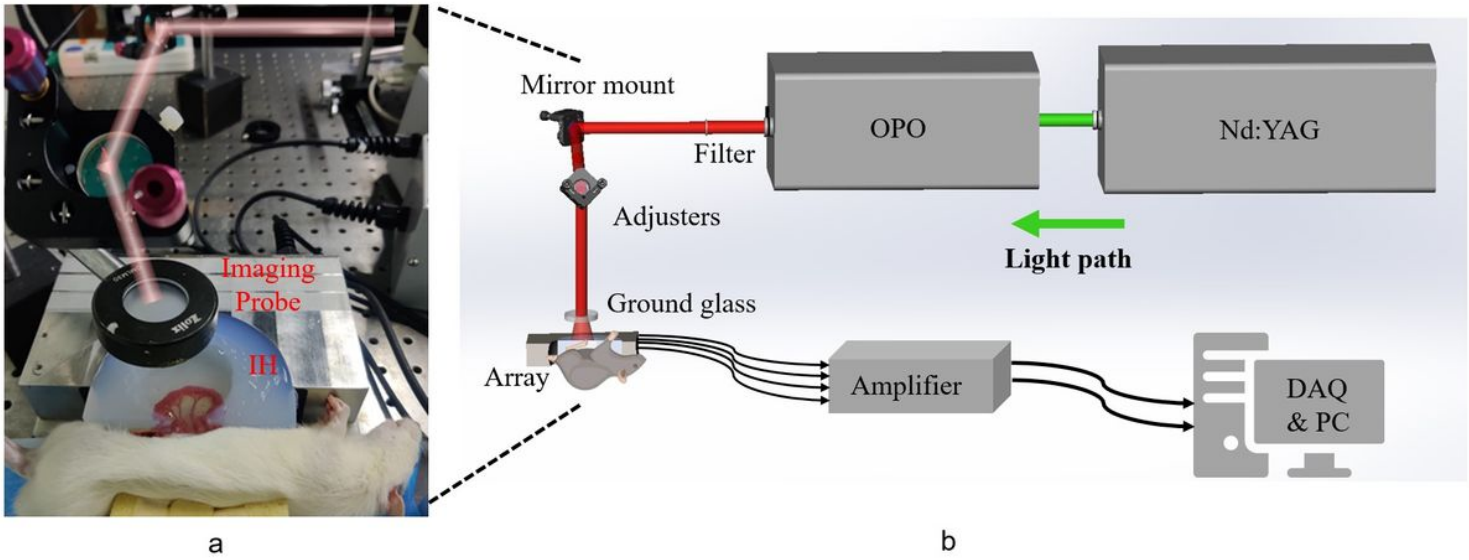

Figure 1

Schematic of the photoacoustic tomography system. (a) Detail of the imaging probe. (b) Schematic of the experimental setup. (DAQ, data acquisition; OPO, optical parametric oscillator; IH, Intestinal holder)

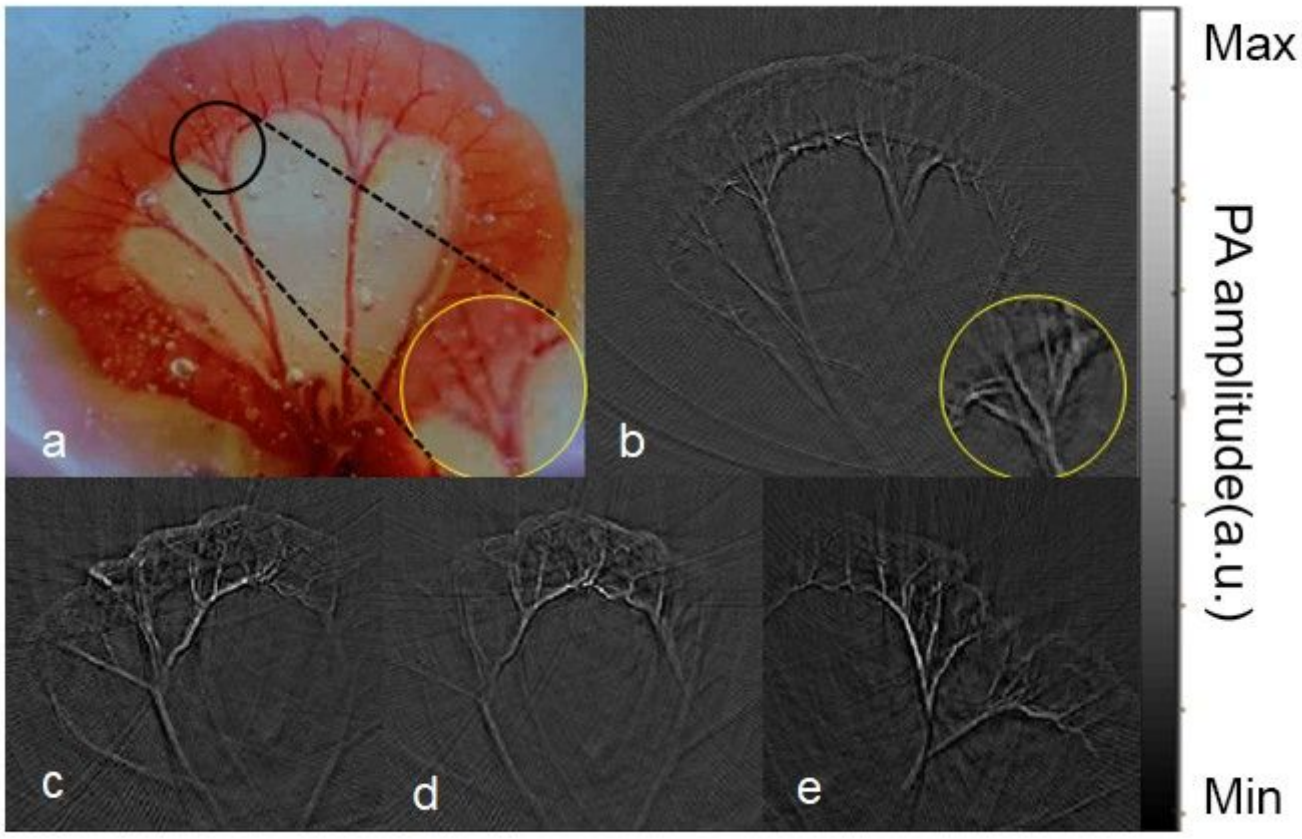

Figure 2

Intestinal images of a rat. (a) Intestinal photograph; (b) Corresponding photoacoustic image. The yellow circle is the enlarged part. Figure 2c, 2d and 2e show three different regions of interest in rat intestinal tissue.

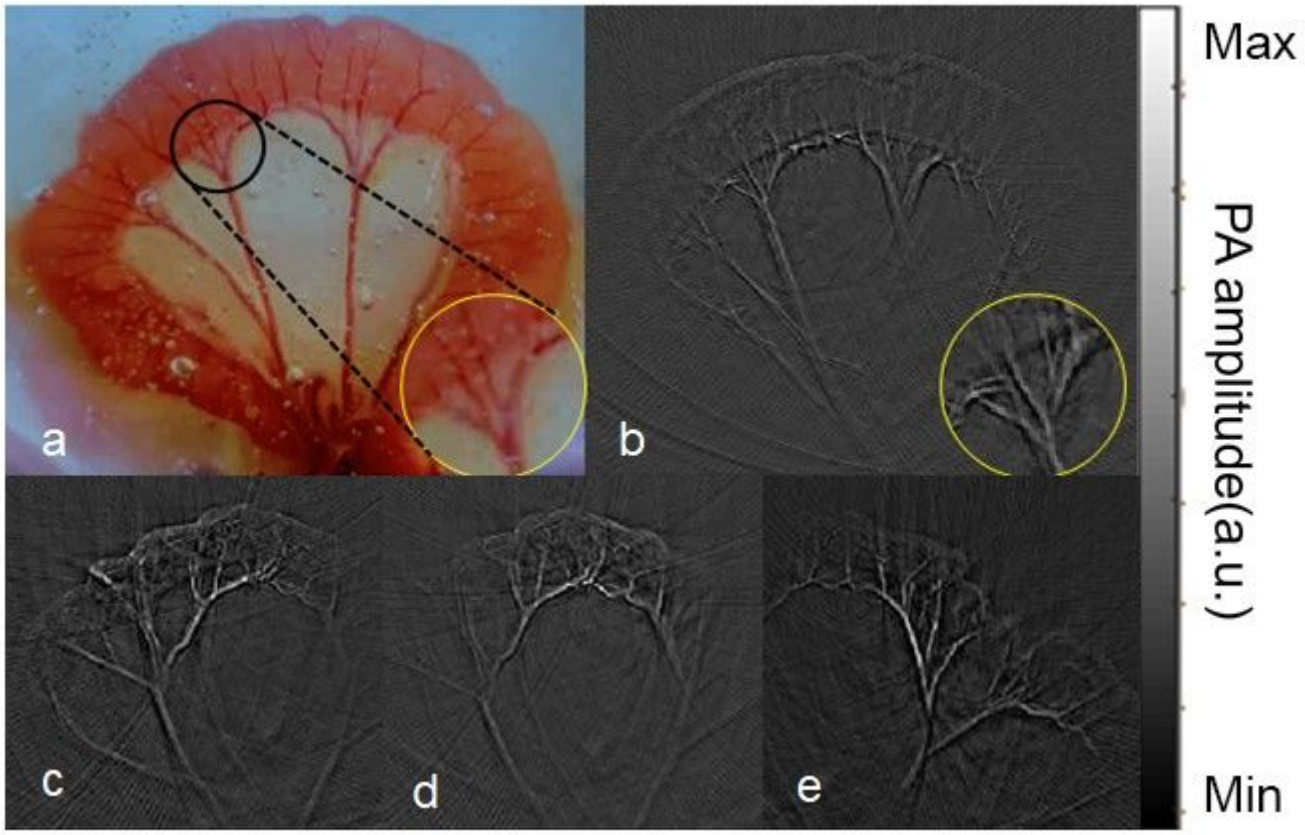

Figure 2

Intestinal images of a rat. (a) Intestinal photograph; (b) Corresponding photoacoustic image. The yellow circle is the enlarged part. Figure 2c, 2d and 2e show three different regions of interest in rat intestinal tissue.

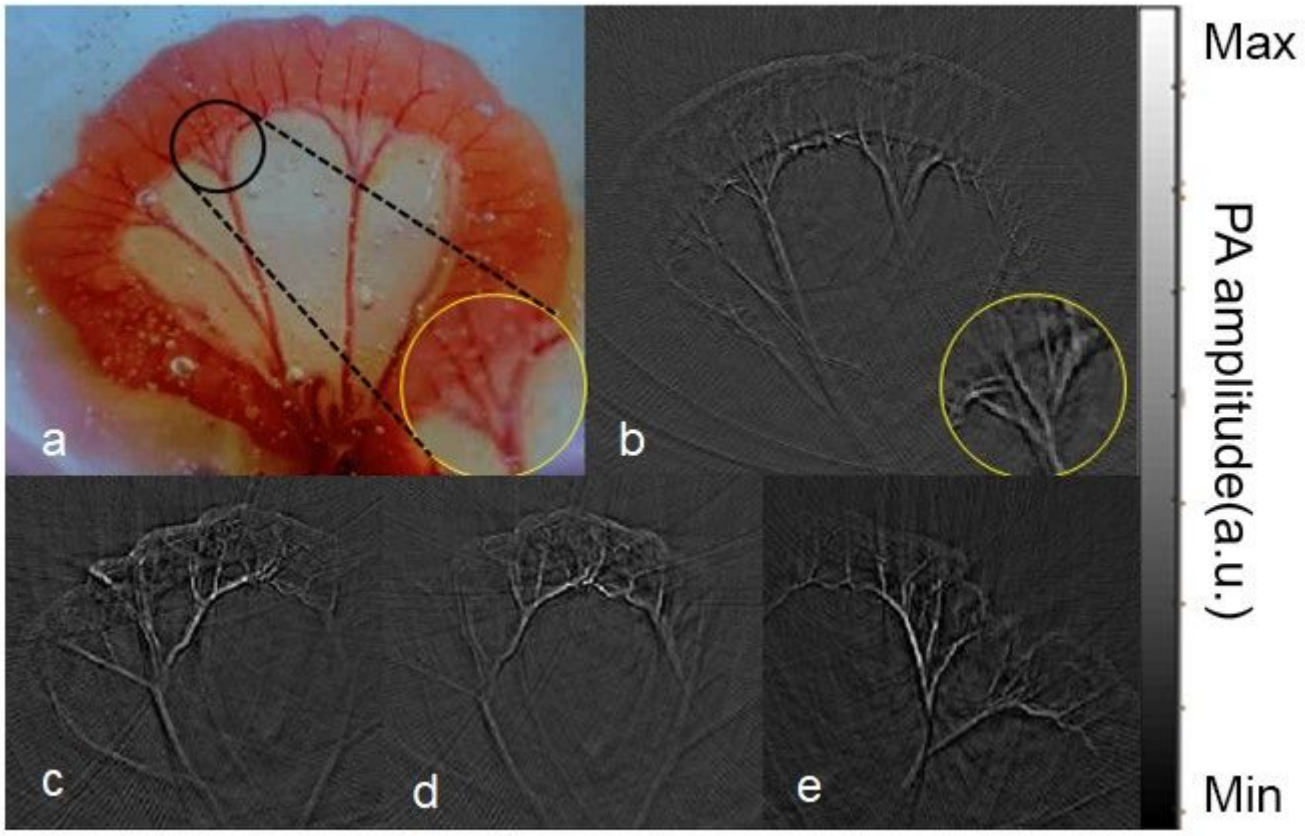

Figure 2

Intestinal images of a rat. (a) Intestinal photograph; (b) Corresponding photoacoustic image. The yellow circle is the enlarged part. Figure 2c, 2d and 2e show three different regions of interest in rat intestinal tissue.

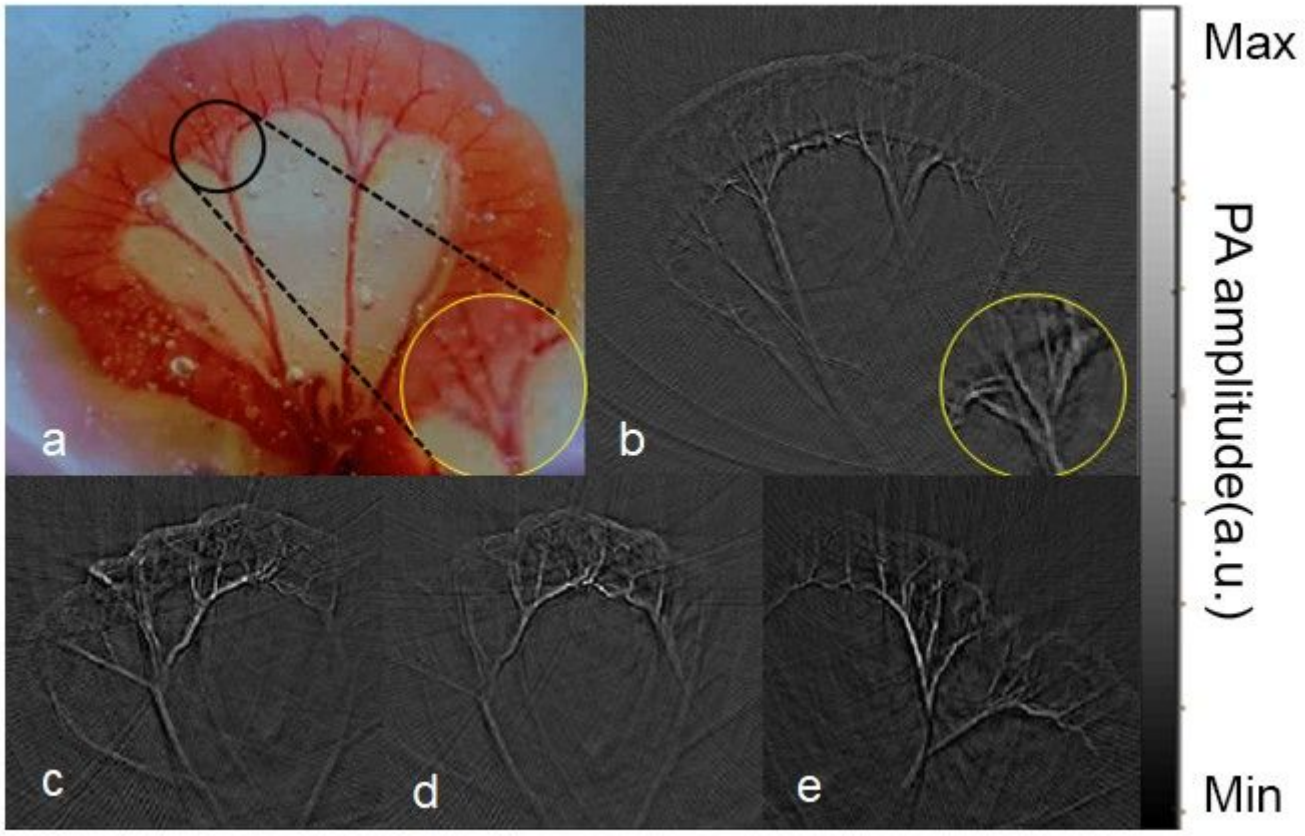

Figure 2

Intestinal images of a rat. (a) Intestinal photograph; (b) Corresponding photoacoustic image. The yellow circle is the enlarged part. Figure 2c, 2d and 2e show three different regions of interest in rat intestinal tissue.

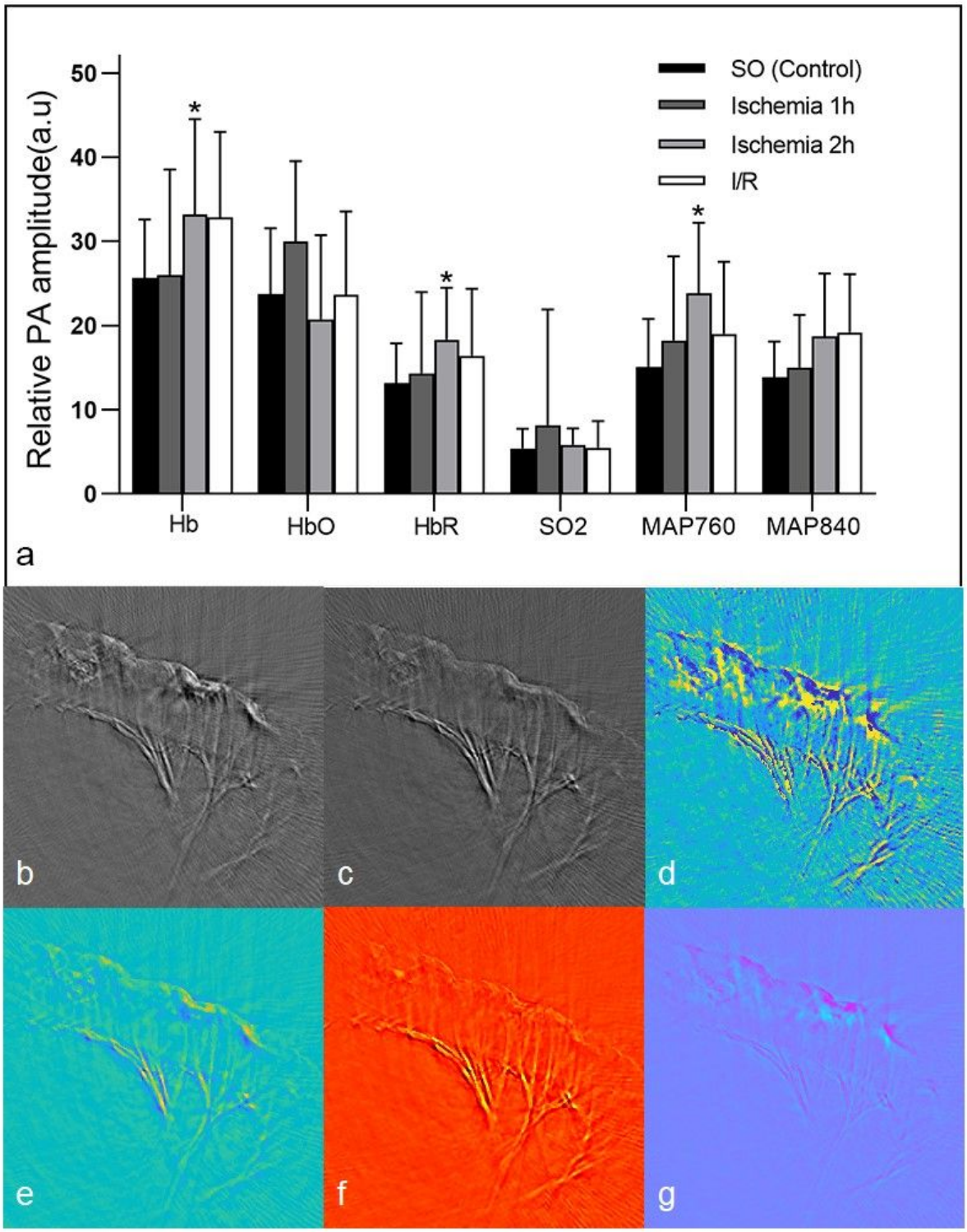

Figure 3

(a) The longitudinal development of six parameters from PAI. Compared with the control group, the signal intensities of Hb, HbR, SO2, MAP 760 and MAP 840 in ischemia group and I/R group were increased in varying degrees, especially in 2 h ischemia group. Figure b, c, d, e, f, g are the parameter diagram of MAP 760, MAP 840, SO2, Hb, HbO and HbR, respectively. (* indicates compared with control $P < 0.05$)

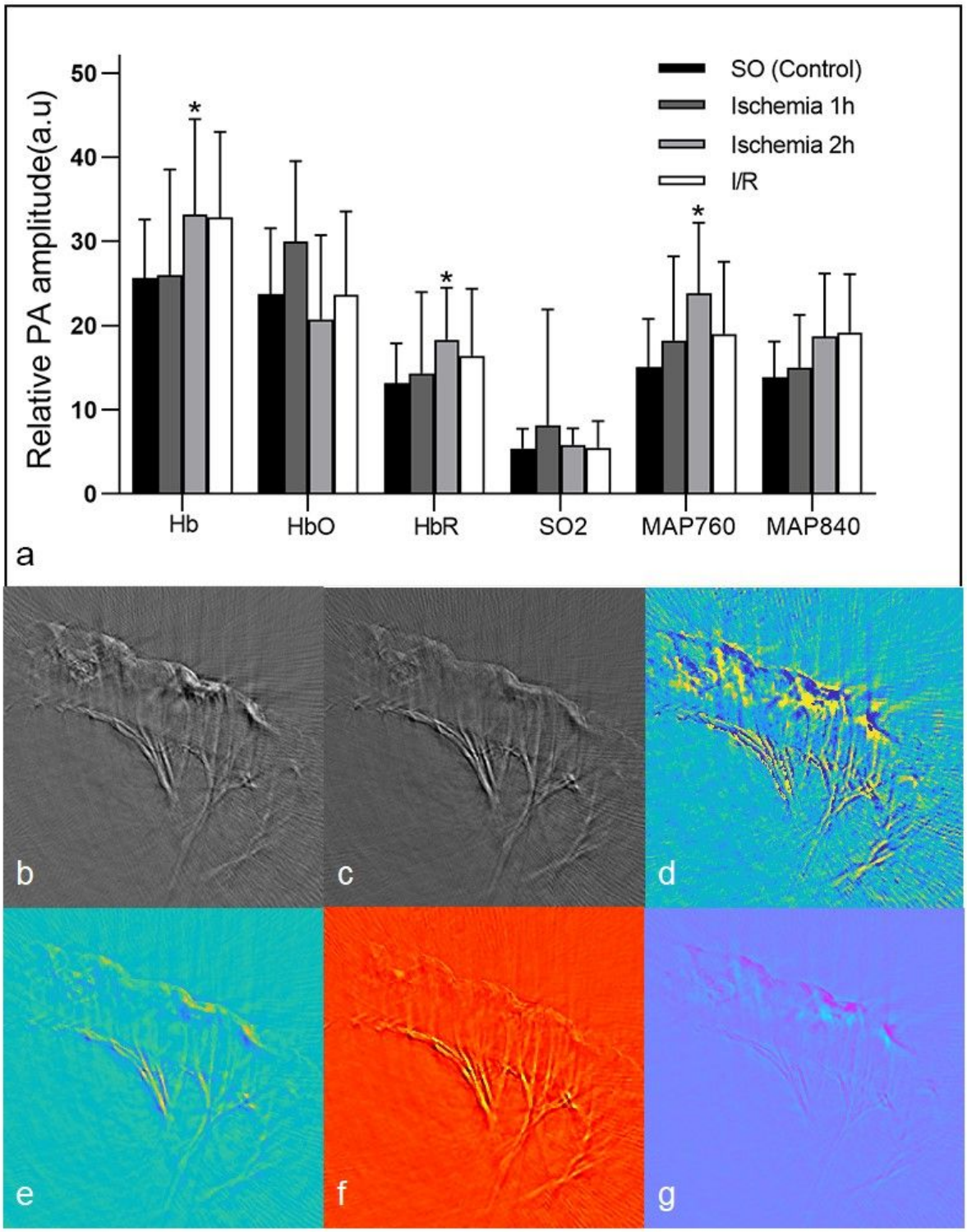

Figure 3

(a) The longitudinal development of six parameters from PAI. Compared with the control group, the signal intensities of Hb, HbR, SO2, MAP 760 and MAP 840 in ischemia group and I/R group were increased in varying degrees, especially in 2 h ischemia group. Figure b, c, d, e, f, g are the parameter diagram of MAP 760, MAP 840, SO2, Hb, HbO and HbR, respectively. (* indicates compared with control $P < 0.05$)

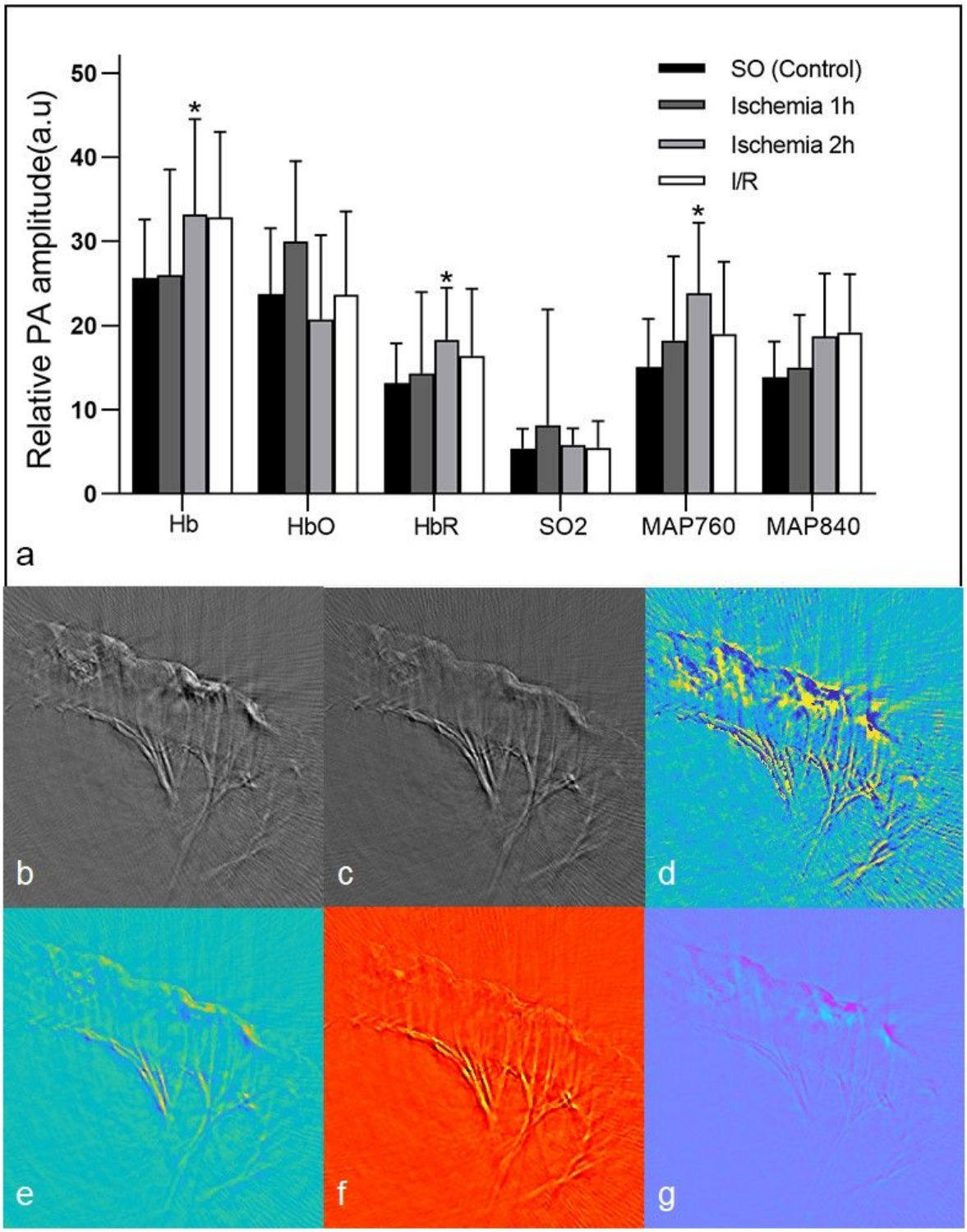

Figure 3

(a) The longitudinal development of six parameters from PAI. Compared with the control group, the signal intensities of Hb, HbR, SO2, MAP 760 and MAP 840 in ischemia group and I/R group were increased in varying degrees, especially in 2 h ischemia group. Figure b, c, d, e, f, g are the parameter diagram of MAP 760, MAP 840, SO2, Hb, HbO and HbR, respectively. (* indicates compared with control $P < 0.05$)

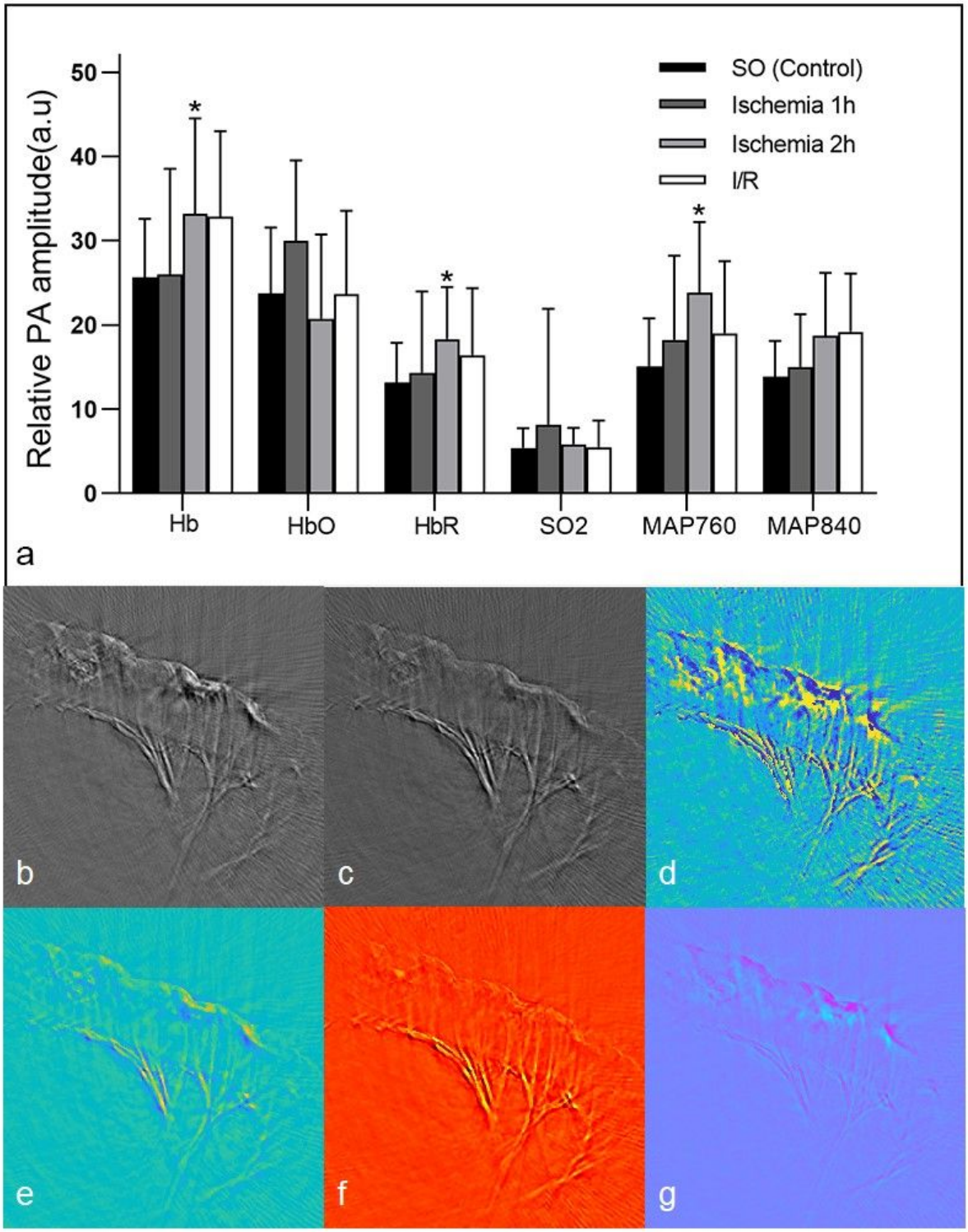

Figure 3

(a) The longitudinal development of six parameters from PAI. Compared with the control group, the signal intensities of Hb, HbR, SO2, MAP 760 and MAP 840 in ischemia group and I/R group were increased in varying degrees, especially in 2 h ischemia group. Figure b, c, d, e, f, g are the parameter diagram of MAP 760, MAP 840, SO2, Hb, HbO and HbR, respectively. (* indicates compared with control $P < 0.05$)

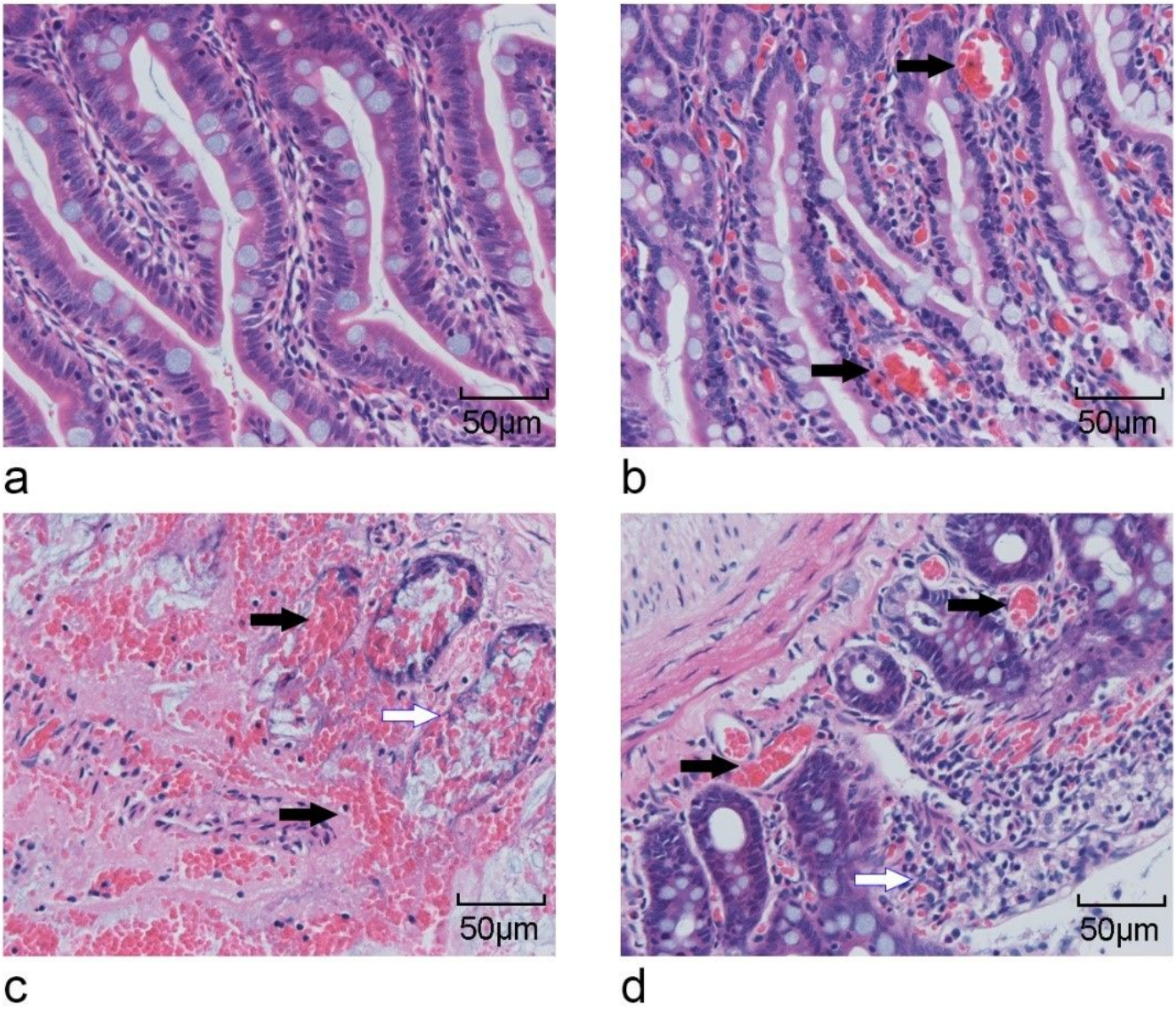

Figure 4

Histopathological changes of intestinal mucosa under light microscope (magnification, ×40). (a) sham-operated group (control group); (b) In 1 h ischemia group, red blood cells were shed from some capillaries; (c) In 2 h ischemia group, the epithelium of intestinal mucosa was exfoliated, and the villi were dissolved and damaged; (d) After 1 h of reperfusion (I/R), the epithelium of some small intestinal mucosa exfoliated and damaged crypt could be seen.

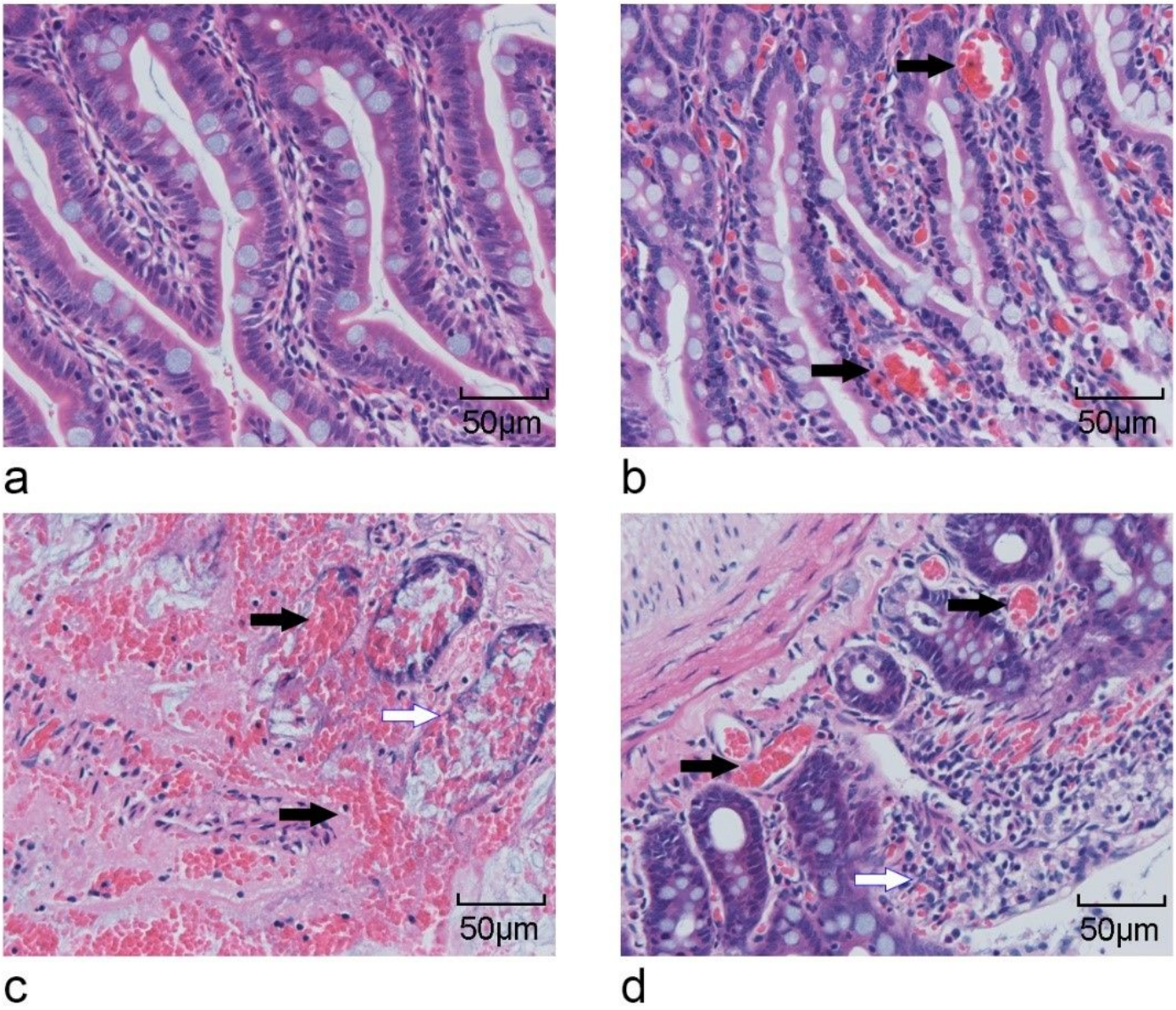

Figure 4

Histopathological changes of intestinal mucosa under light microscope (magnification, ×40). (a) sham-operated group (control group); (b) In 1 h ischemia group, red blood cells were shed from some capillaries; (c) In 2 h ischemia group, the epithelium of intestinal mucosa was exfoliated, and the villi were dissolved and damaged; (d) After 1 h of reperfusion (I/R), the epithelium of some small intestinal mucosa exfoliated and damaged crypt could be seen.

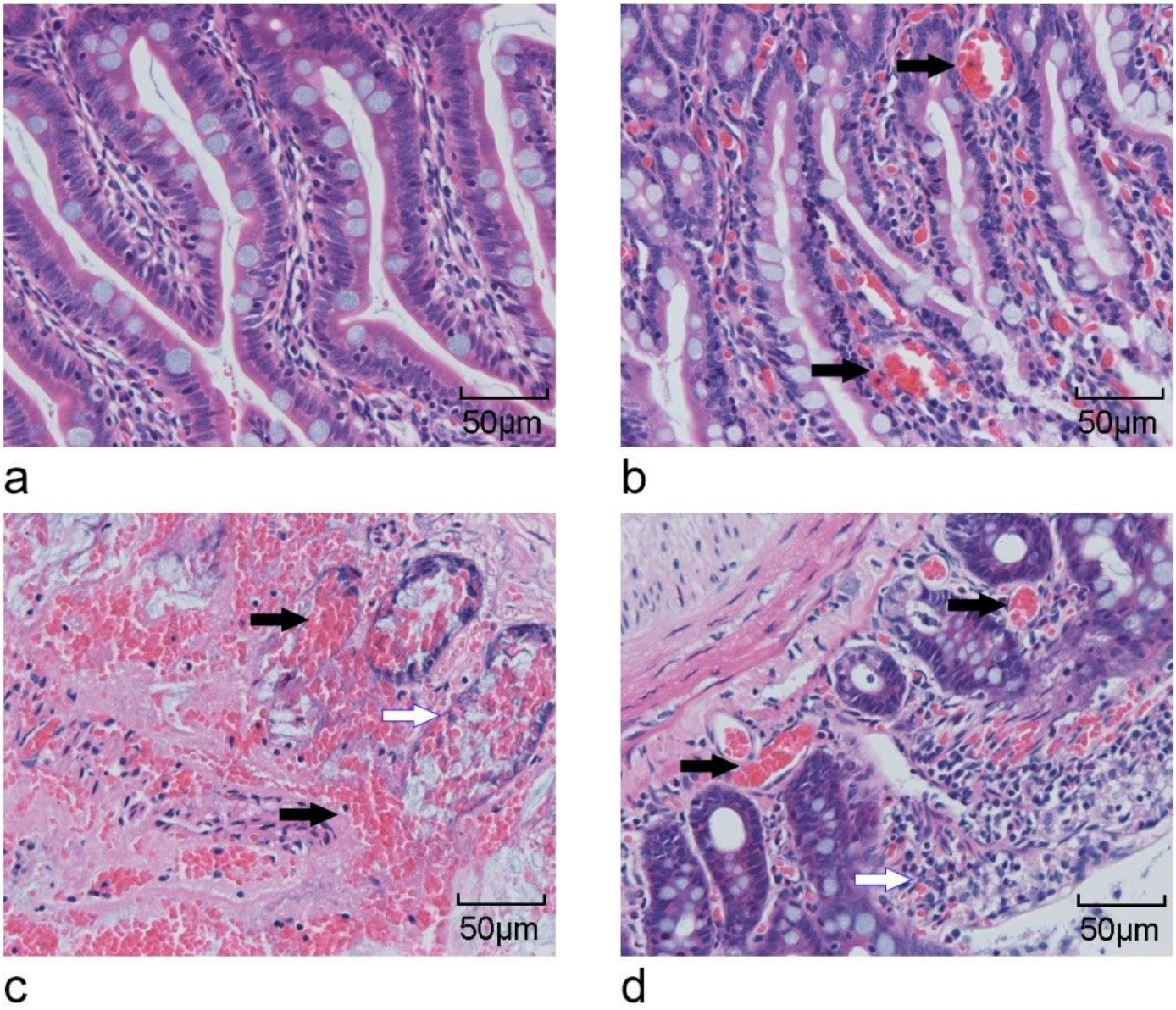

Figure 4

Histopathological changes of intestinal mucosa under light microscope (magnification, ×40). (a) sham-operated group (control group); (b) In 1 h ischemia group, red blood cells were shed from some capillaries; (c) In 2 h ischemia group, the epithelium of intestinal mucosa was exfoliated, and the villi were dissolved and damaged; (d) After 1 h of reperfusion (I/R), the epithelium of some small intestinal mucosa exfoliated and damaged crypt could be seen.

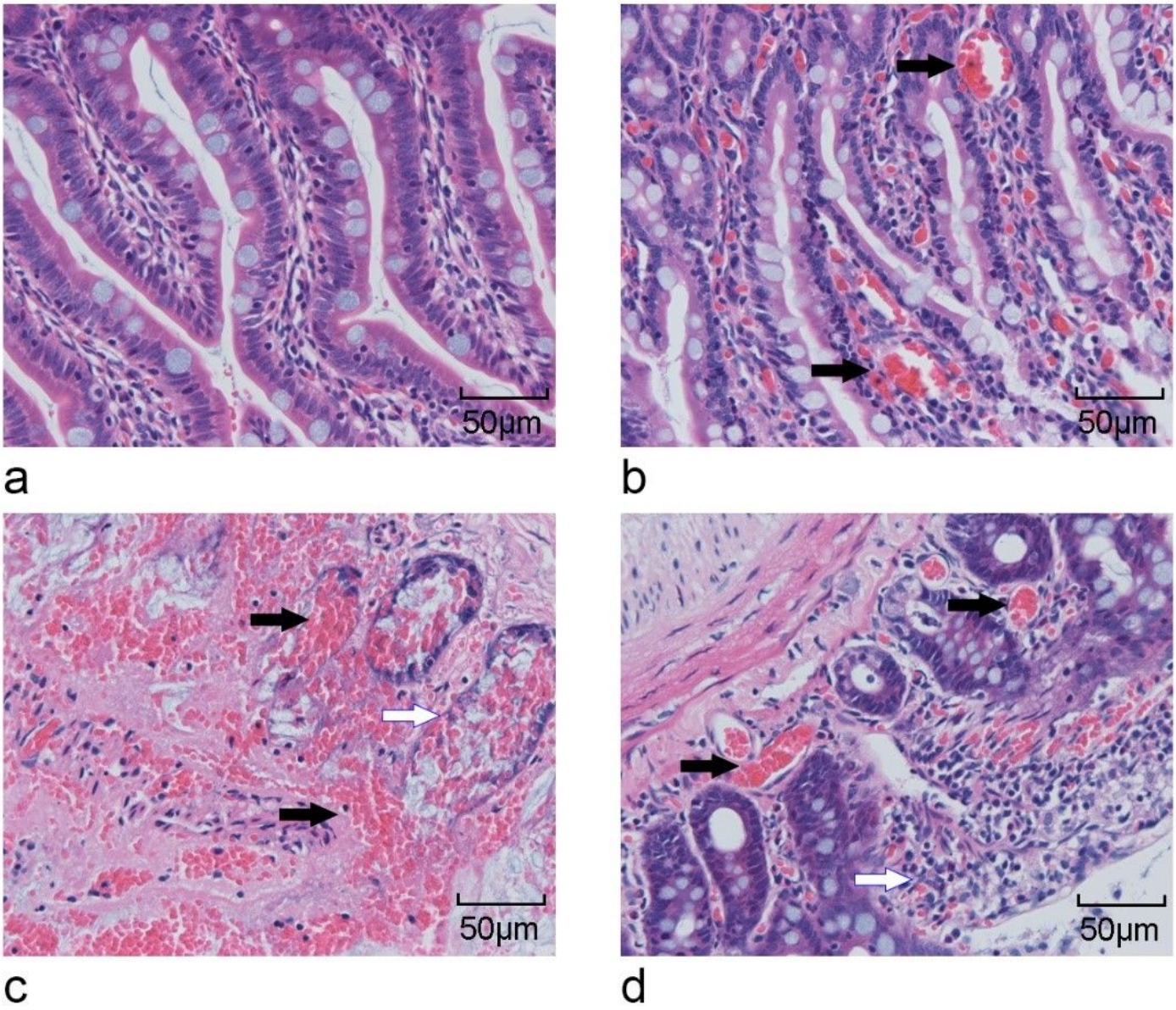

Figure 4

Histopathological changes of intestinal mucosa under light microscope (magnification, ×40). (a) sham-operated group (control group); (b) In 1 h ischemia group, red blood cells were shed from some capillaries; (c) In 2 h ischemia group, the epithelium of intestinal mucosa was exfoliated, and the villi were dissolved and damaged; (d) After 1 h of reperfusion (I/R), the epithelium of some small intestinal mucosa exfoliated and damaged crypt could be seen.

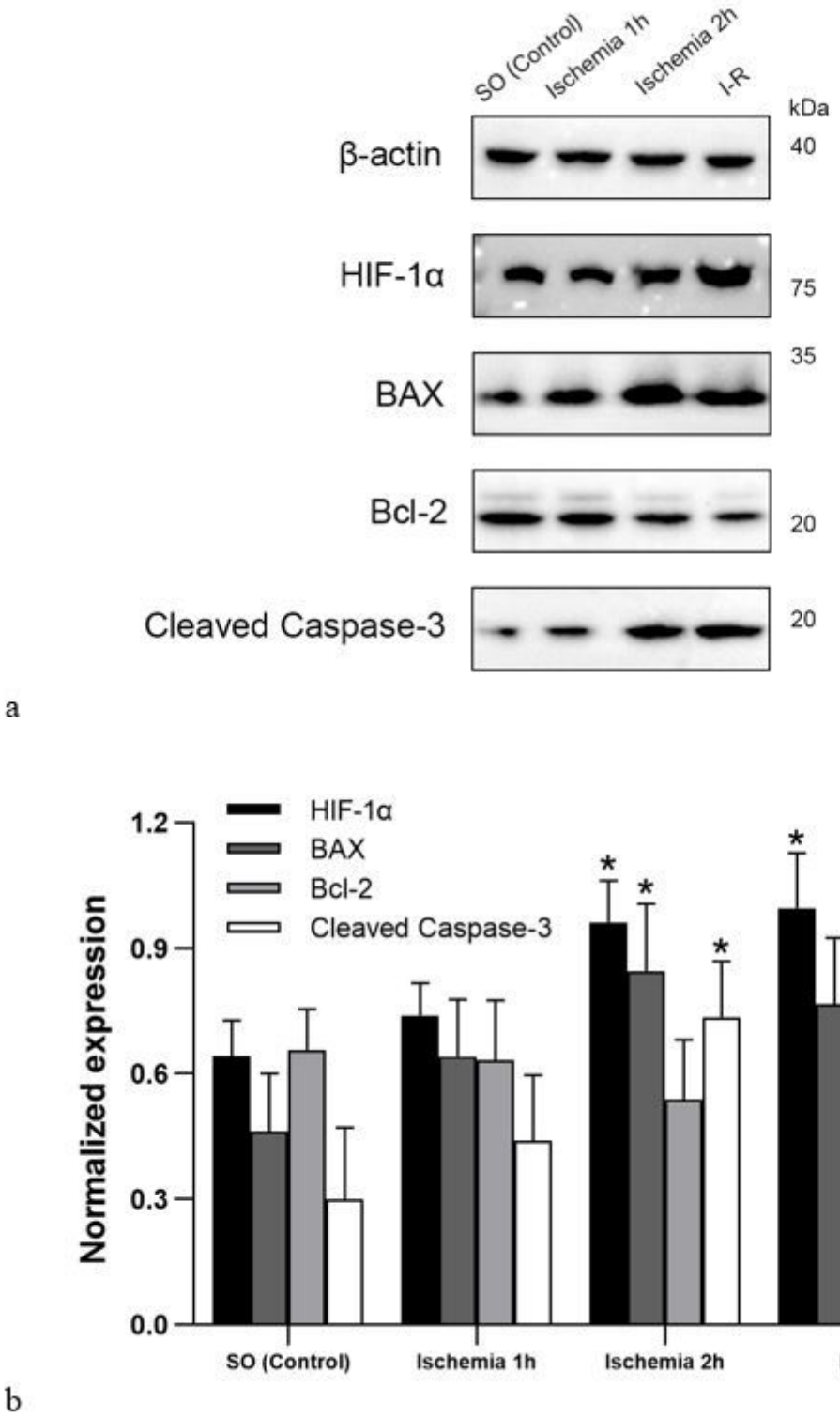

Figure 5

Expression of HIF, Bax, Bcl-2 and Cleaved Caspase-3 in intestinal mucosa of rats with intestinal ischemia-reperfusion injury. a There was no significant difference in the expression of inflammatory bodies and apoptosis between the two groups. The level of cleaved caspase-3 in 2 h ischemia group and IR group was significantly higher than that in control group ($P < 0.05$), and BAX level in 2 h ischemia group was significantly higher than that in control group ($P < 0.01$). The level of HIF-1a increased in 2 h ischemia

group and I/R group (P < 0.05). b The histogram after quantitative analysis by ImageJ software. (* indicates compared with control P < 0.05)

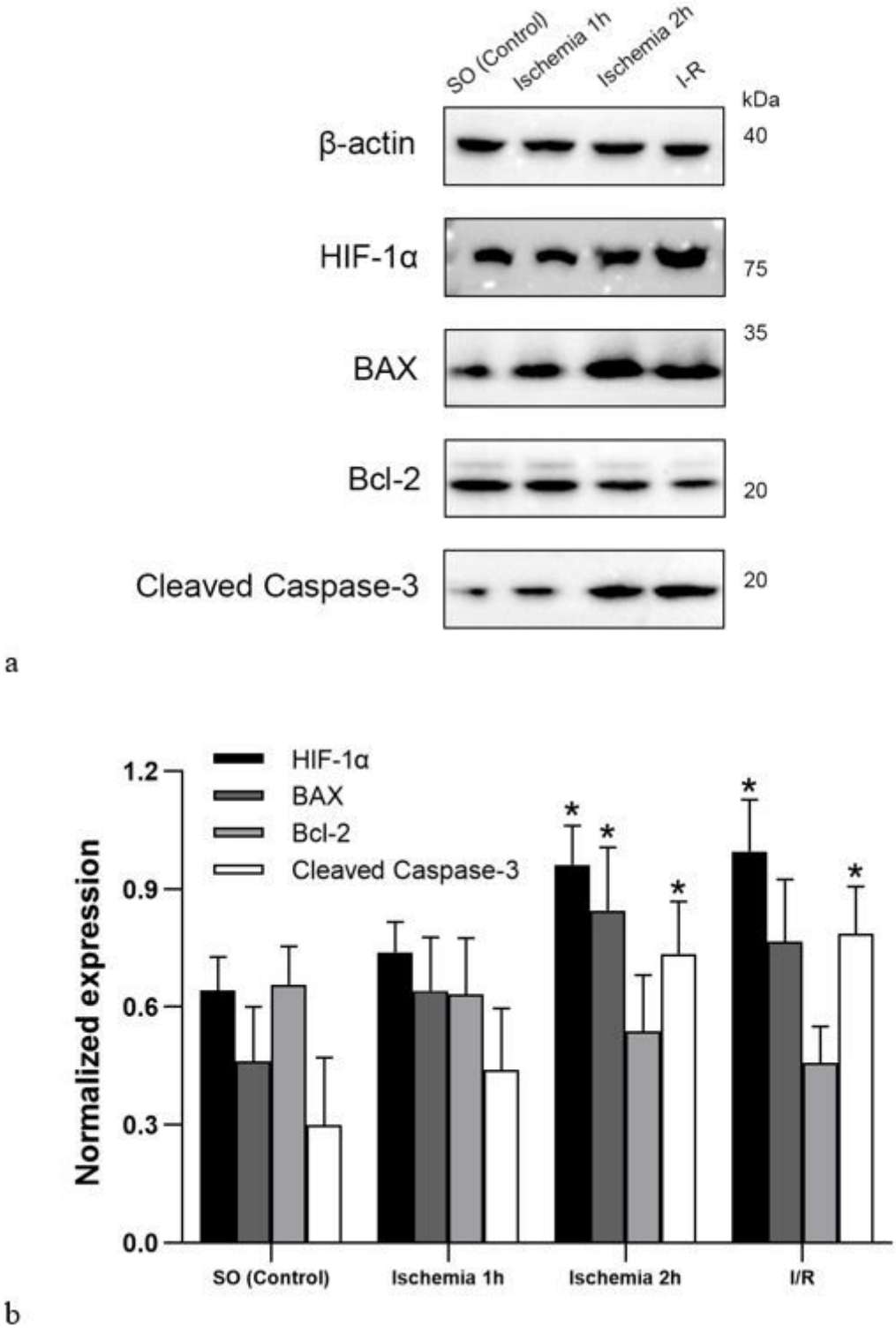

Figure 5

Expression of HIF, Bax, Bcl-2 and Cleaved Caspase-3 in intestinal mucosa of rats with intestinal ischemia-reperfusion injury. a There was no significant difference in the expression of inflammatory bodies and apoptosis between the two groups. The level of cleaved caspase-3 in 2 h ischemia group and IR group

was significantly higher than that in control group (P < 0.05), and BAX level in 2 h ischemia group was significantly higher than that in control group (P < 0.01). The level of HIF-1a increased in 2 h ischemia group and I/R group (P < 0.05). b The histogram after quantitative analysis by ImageJ software. (* indicates compared with control P < 0.05)

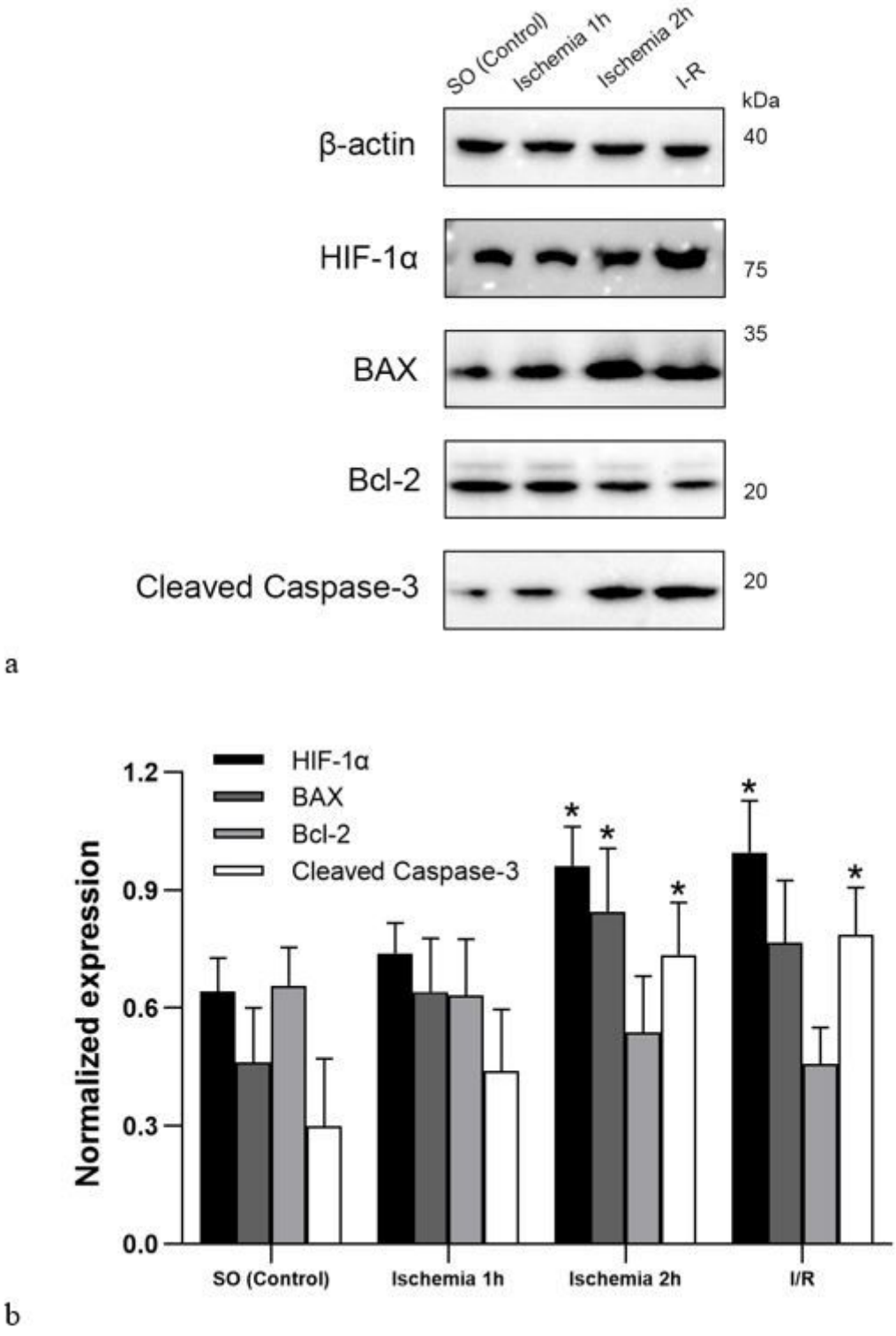

Figure 5

Expression of HIF, Bax, Bcl-2 and Cleaved Caspase-3 in intestinal mucosa of rats with intestinal ischemia-reperfusion injury. a There was no significant difference in the expression of inflammatory bodies and apoptosis between the two groups. The level of cleaved caspase-3 in 2 h ischemia group and IR group was significantly higher than that in control group ($P < 0.05$), and BAX level in 2 h ischemia group was significantly higher than that in control group ($P < 0.01$). The level of HIF-1a increased in 2 h ischemia group and I/R group ($P < 0.05$). b The histogram after quantitative analysis by ImageJ software. (* indicates compared with control $P < 0.05$)

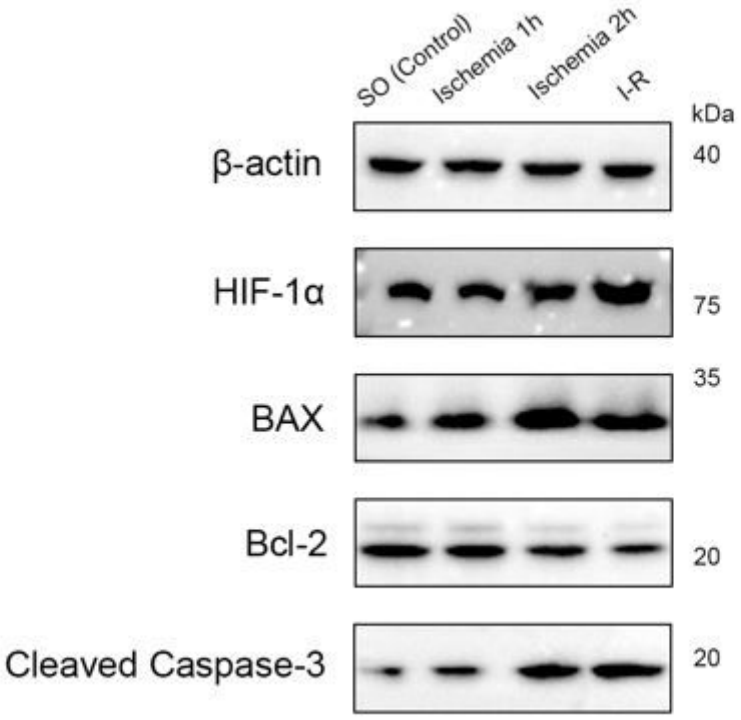

a

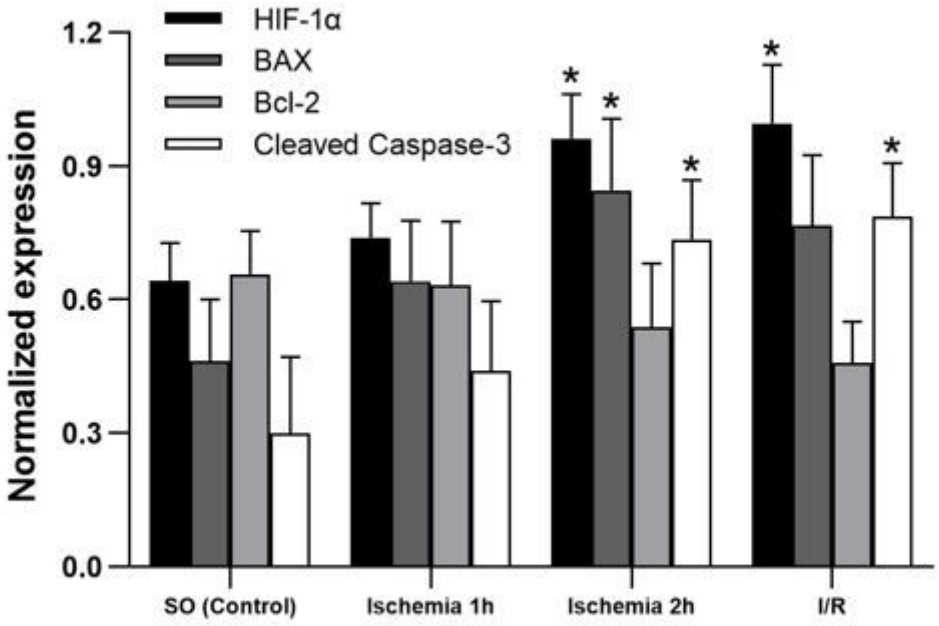

b

Figure 5

Expression of HIF, Bax, Bcl-2 and Cleaved Caspase-3 in intestinal mucosa of rats with intestinal ischemia-reperfusion injury. a There was no significant difference in the expression of inflammatory bodies and apoptosis between the two groups. The level of cleaved caspase-3 in 2 h ischemia group and IR group was significantly higher than that in control group ($P < 0.05$), and BAX level in 2 h ischemia group was significantly higher than that in control group ($P < 0.01$). The level of HIF-1a increased in 2 h ischemia group and I/R group ($P < 0.05$). b The histogram after quantitative analysis by ImageJ software. (* indicates compared with control $P < 0.05$)

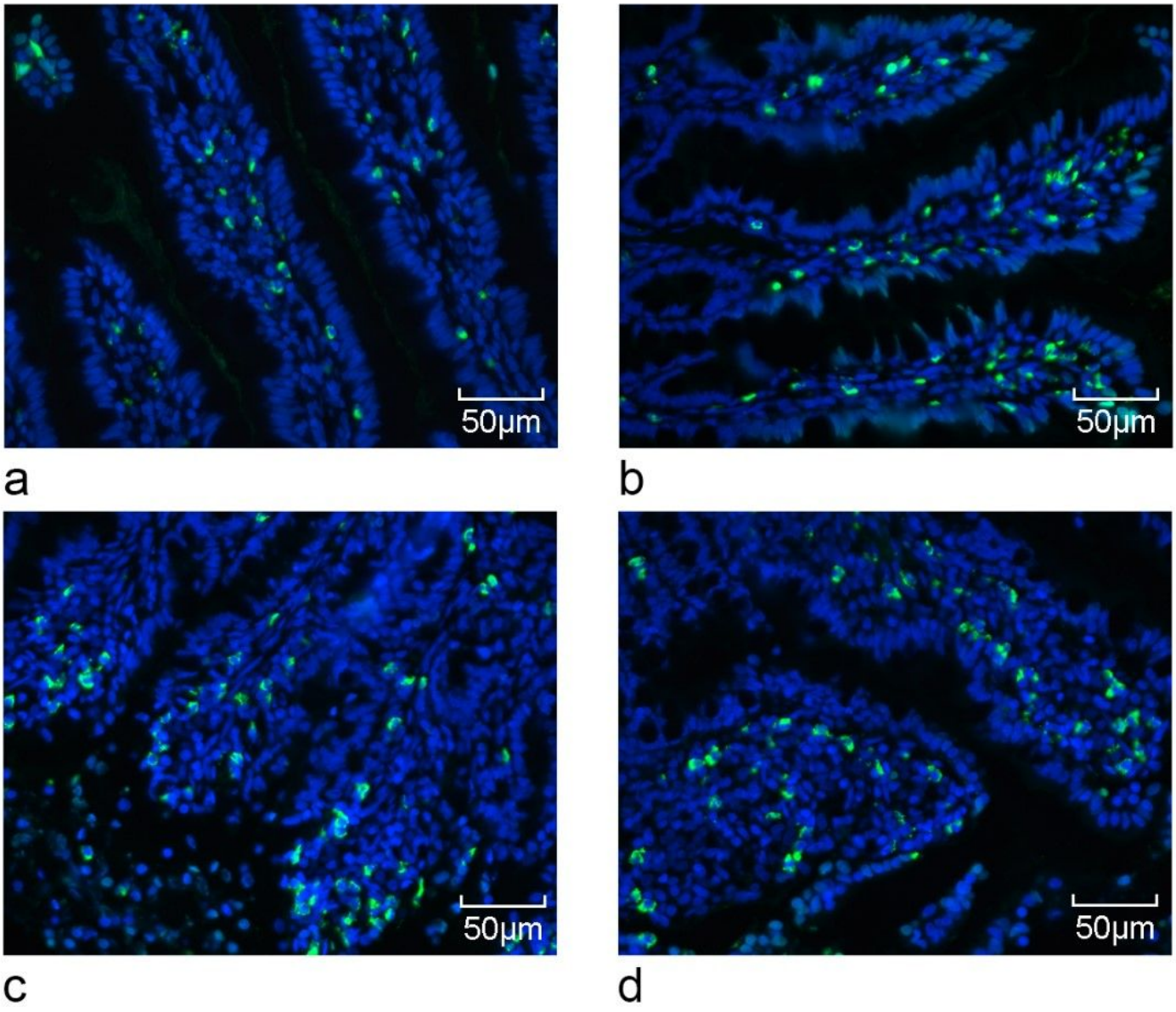

Figure 6

TUNEL labeling of apoptotic nuclei (magnification, ×40). (a) sham-operated group; (b) 1 h ischemia group; (c) 2 h ischemia group; (d) Ischemia reperfusion group (I/R). The apoptosis of intestinal mucosal

cells was the most serious in 2 h ischemia group.

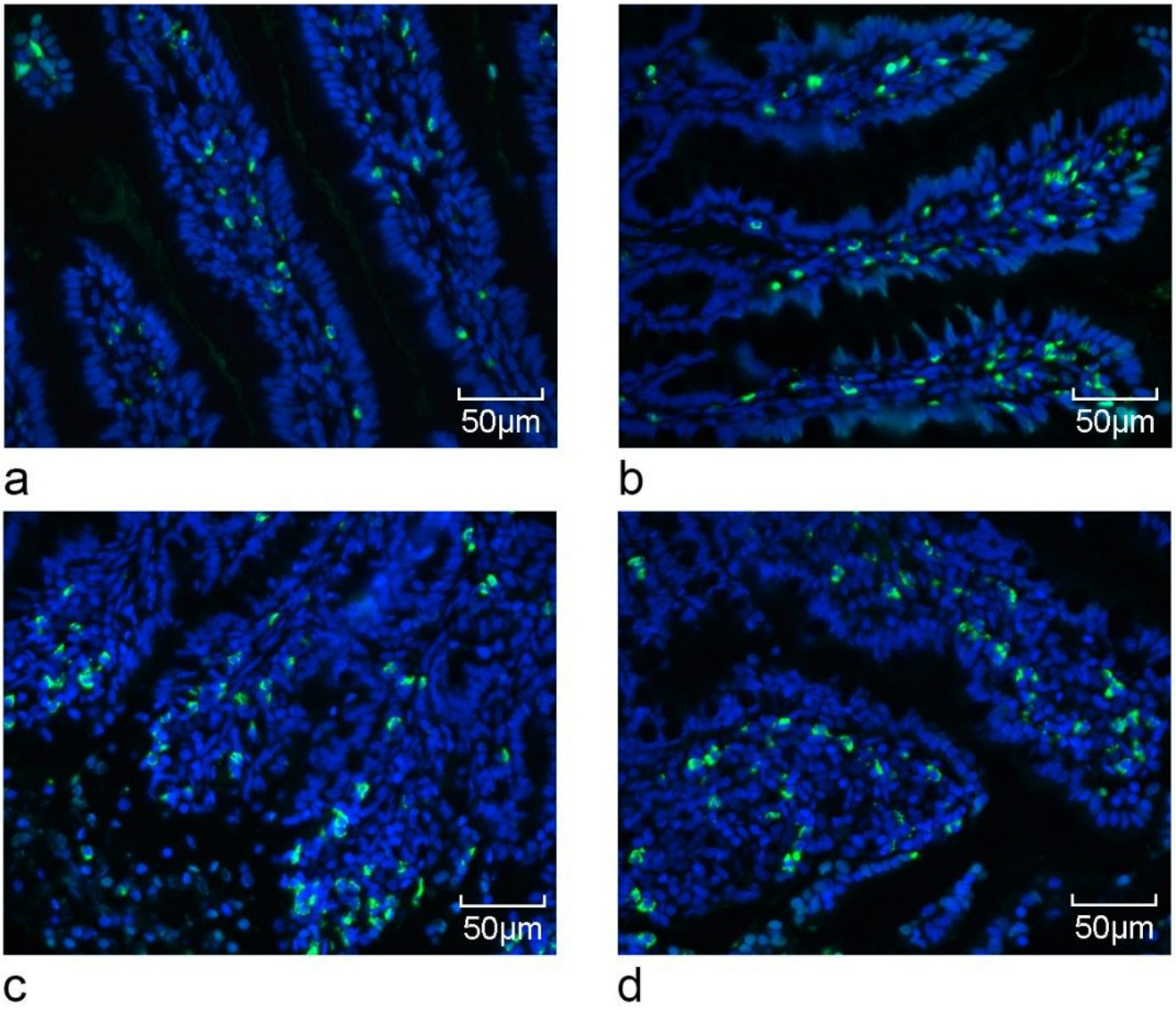

Figure 6

TUNEL labeling of apoptotic nuclei (magnification, ×40). (a) sham-operated group; (b) 1 h ischemia group; (c) 2 h ischemia group; (d) Ischemia reperfusion group (I/R). The apoptosis of intestinal mucosal cells was the most serious in 2 h ischemia group.

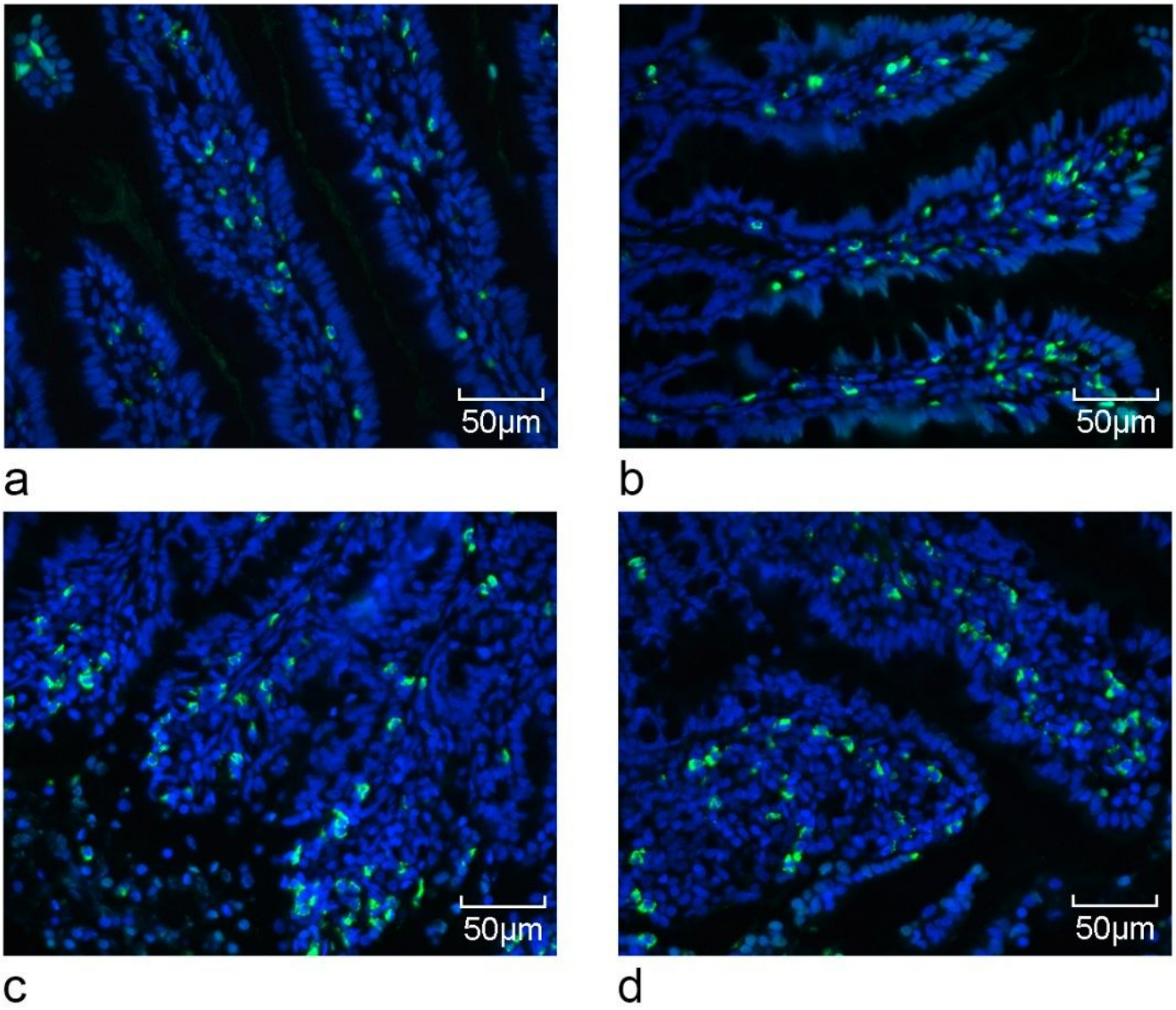

Figure 6

TUNEL labeling of apoptotic nuclei (magnification, ×40). (a) sham-operated group; (b) 1 h ischemia group; (c) 2 h ischemia group; (d) Ischemia reperfusion group (I/R). The apoptosis of intestinal mucosal cells was the most serious in 2 h ischemia group.

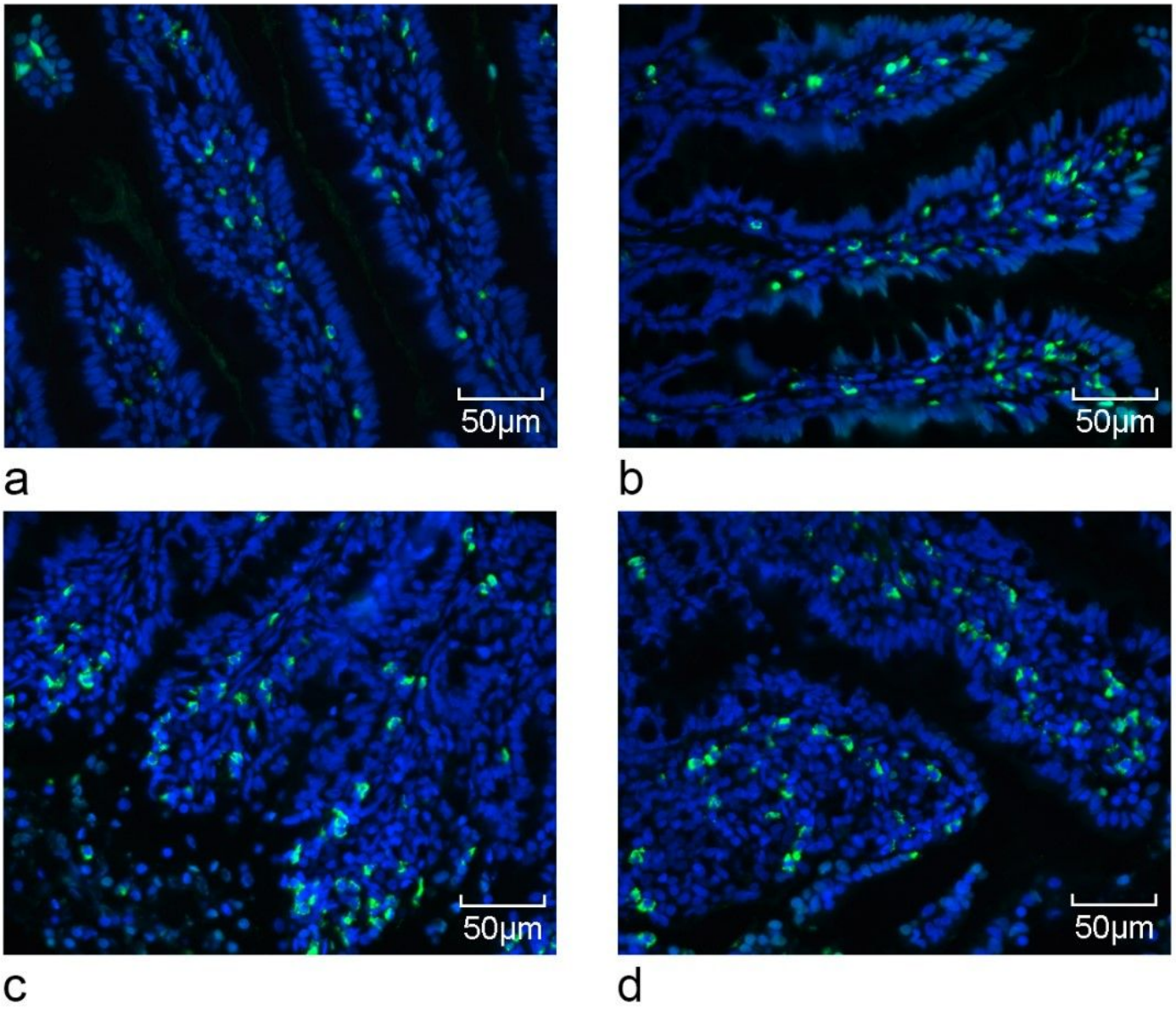

Figure 6

TUNEL labeling of apoptotic nuclei (magnification, ×40). (a) sham-operated group; (b) 1 h ischemia group; (c) 2 h ischemia group; (d) Ischemia reperfusion group (I/R). The apoptosis of intestinal mucosal cells was the most serious in 2 h ischemia group.